Appl. Statist. (2020)
69, *Part* 5, *pp.* 1–39

Linear mixed effects models for non-Gaussian continuous repeated measurement data

Özgür Asar,

Acıbadem Mehmet Ali Aydınlar University, İstanbul, Turkey

David Bolin,

King Abdullah University of Science and Technology, Thuwal, Saudi Arabia, and University of Gothenburg, Sweden

Peter J. Diggle,

Lancaster University, UK

and Jonas Wallin

Lund University, Lund, Sweden

[*Read before* The Royal Statistical Society *at a meeting organized by the* Research Section on *Wednesday, May 13th, 2020*, Professor G. P. Nason *in the Chair*]

Summary. We consider the analysis of continuous repeated measurement outcomes that are collected longitudinally. A standard framework for analysing data of this kind is a linear Gaussian mixed effects model within which the outcome variable can be decomposed into fixed effects, time invariant and time-varying random effects, and measurement noise. We develop methodology that, for the first time, allows any combination of these stochastic components to be non-Gaussian, using multivariate normal variance–mean mixtures. To meet the computational challenges that are presented by large data sets, i.e. in the current context, data sets with many subjects and/or many repeated measurements per subject, we propose a novel implementation of maximum likelihood estimation using a computationally efficient subsampling-based stochastic gradient algorithm. We obtain standard error estimates by inverting the observed Fisher information matrix and obtain the predictive distributions for the random effects in both filtering (conditioning on past and current data) and smoothing (conditioning on all data) contexts. To implement these procedures, we introduce an `R` package: `ngme`. We reanalyse two data sets, from cystic fibrosis and nephrology research, that were previously analysed by using Gaussian linear mixed effects models.

Keywords: Heavy-tailedness; Latent effects; Longitudinal data; Multivariate analysis; Non-normal distributions; Skewness; Stochastic approximation; Tail data

1. Introduction

This paper is concerned with the analysis of real-valued *repeated measurement* data that are collected through time, also known as *longitudinal* data. The basic data structure is that repeated measurements of an *outcome variable* are made on each of a number of *subjects* at each of a number of *follow-up times*, which are not necessarily the same for all subjects, with explanatory

Address for correspondence: Jonas Wallin, Lund Universitet Ekonomihogskolan—Statistika, Tycho Brahes vag 1, Lund 220 07, Sweden.
E-mail: jonas.wallin@stat.lu.se

0035–9254/20/69000

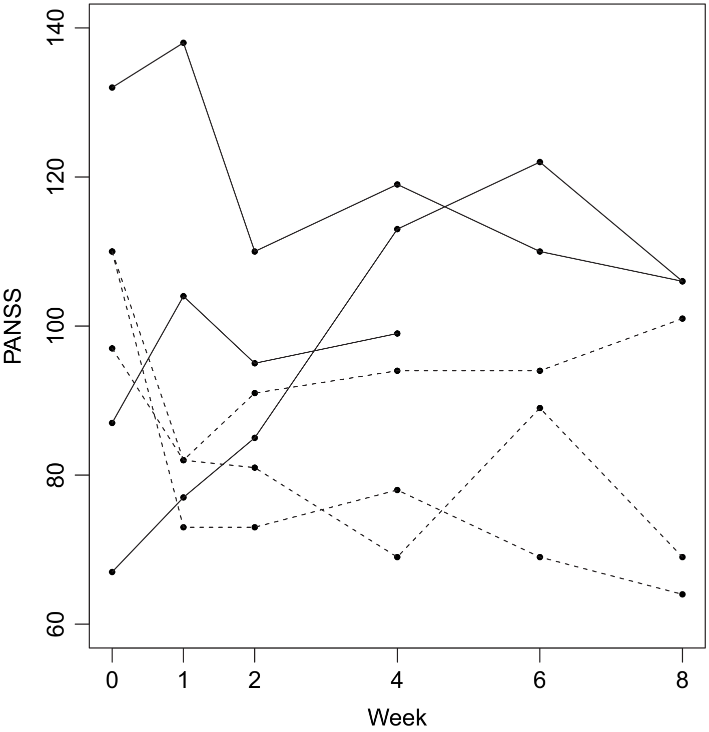

Fig. 1. Data on six patients in a randomized trial of drug therapies for schizophrenia (the outcome variable, PANSS (positive and negative syndrome scale), is a questionnaire-based instrument for assessing the severity of a patient's condition): ———, patients from the placebo treatment arm; - - - - -, patients from the active treatment arm

variables or *covariates* of two kinds also available: *baseline* covariates attached to subjects, and *longitudinal* covariates attached to individual outcomes. We write Y_{ij} for the jth measurement of the outcome on the ith subject, t_{ij} for the corresponding follow-up time, $\mathbf{a}_i$ for the matrix of baseline covariates that are associated with the ith subject and $\mathbf{x}_{ij}$ for the matrix of longitudinal covariates that are attached to the jth measurement on the ith subject.

Fig. 1 shows a simple example, taken from a randomized trial of drug treatments for schizophrenia, in which the outcome variable is a measure of each subject's mental state at times 0, 1, 2, 4, 6 and 8 weeks after randomization to one of two different drug therapies: placebo *versus* active treatment. Here, a_i is a scalar treatment indicator, whereas the general pattern of decreasing responses over time suggests a quadratic trend; hence $\mathbf{x}_{ij}$ consists of t_{ij} and t_{ij}^2. Fig. 1 shows data from three subjects in each of the two treatment arms; the complete trial included 88 subjects in the placebo group and 435 subjects distributed across five active treatment arms (Henderson *et al.*, 2000). This example shows several features that are typical of studies of this kind: the outcome variable, the PANSS-score (positive and negative syndrome scale) (Kay *et al.*, 1987), is an imperfect measurement instrument for the underlying process of interest, namely each subject's state of mental health at the time of measurement; the outcome variable exhibits stochastic variation both between subjects and between follow-up times within subjects; questions of interest include *estimation* of parameters that define the mean response profiles of the underlying process over time and *prediction* of the trajectory of the process for an individual subject.

Most of the very extensive literature on statistical methods for data of this kind uses either a Gaussian model or, if the inferential goal is restricted to parameter estimation, a set of estimating equations; textbook accounts include Verbeke and Molenberghs (2001), Diggle *et al.* (2002) and Fitzmaurice *et al.* (2011). In this paper, we present methodology for handling repeated measurement data that exhibit long-tailed or skewed departure from Gaussian distributional assumptions.

In Section 2, we review the literature on existing approaches to Gaussian and non-Gaussian modelling of real-valued repeated measurement data. In Section 3, we set out our proposed class of non-Gaussian models. In Section 4, we describe a computationally fast method for likelihood-based inference. Section 5 describes a method for validating the distributional assumptions of the models considered. Section 6 describes two applications. In the first of these, the scientific focus is on estimation of mean response profiles, whereas in the second the focus is on realtime individual level prediction. Section 7 presents the results from two simulation studies and Section 8 describes our R package, `ngme`, that implements the new methodology. In Section 9, we discuss some potential extensions, including models for categorical or count data (Molenberghs and Verbeke, 2005) and joint modelling of repeated measurement and time-to-event data (Rizopoulos, 2012). Technical details are presented in the appendices.

2. Literature review

2.1. Gaussian models for real-valued repeated measurement data

Laird and Ware (1982) were the first to consider modelling repeated measurements as noisy versions of underlying signals that can be decomposed into fixed effects $\mathbf{a}_i^{\mathrm{T}}\boldsymbol{\alpha}+\mathbf{x}_{ij}^{\mathrm{T}}\boldsymbol{\beta}$ and random effects $\mathbf{d}_{ij}^{\mathrm{T}}\mathbf{U}_i$, leading to the mixed effects model

$$Y_{ij}=\mathbf{a}_i^{\mathrm{T}}\boldsymbol{\alpha}+\mathbf{x}_{ij}^{\mathrm{T}}\boldsymbol{\beta}+\mathbf{d}_{ij}^{\mathrm{T}}\mathbf{U}_i+\sigma Z_{ij},\qquad j=1,\ldots,n_i,\quad i=1,\ldots,m, \tag{1}$$

where n_i is the number of measurements on the ith subject, m is the number of subjects, the individual level $\mathbf{U}_i$ are mutually independent, zero-mean multivariate normal, $\mathbf{U}_i \sim N(\mathbf{0},\boldsymbol{\Sigma})$ and the Z_{ij} are mutually independent $N(0,1)$.

A widely used special case of model (1) is the 'random-intercept and random-slope' model in which each subject's random effect is a linear function of time. This model is very useful when the data contain only a small number of repeated measurements per individual. With longer sequences, the assumption that individual random-effect trajectories can be approximated by straight lines becomes implausible, because of non-linearities in the trajectories. Diggle (1988) proposed adding to the model a *time-varying* random-effect term $W_i(t)$, specified as a stationary stochastic process. Taylor *et al.* (1994) and Diggle *et al.* (2015) later considered non-stationary options for $W_i(t)$. The general specification for models of this kind is that

$$Y_{ij}=\mathbf{a}_i^{\mathrm{T}}\boldsymbol{\alpha}+\mathbf{x}_{ij}^{\mathrm{T}}\boldsymbol{\beta}+\mathbf{d}_{ij}^{\mathrm{T}}\mathbf{U}_i+W_i(t_{ij})+\sigma Z_{ij}, \tag{2}$$

where, in addition to the notation that has already been introduced, the $W_i(t)$ are independent copies of a continuous time zero-mean Gaussian process with covariance function $\gamma(t,t')=\operatorname{cov}\{W_i(t),W_i(t')\}$. We consider the elements of both the $\mathbf{a}_i$ and $\mathbf{x}_{ij}$ to be prespecified constants. This implicitly assumes, in particular, that, if any time-varying covariate is not prespecified, it is stochastically independent of all other terms in the model; hence conditioning on it is innocuous. We can then drop the term $\mathbf{a}_i^{\mathrm{T}}\boldsymbol{\alpha}$ in model (2) by allowing elements of $\mathbf{x}_{ij}$ to take identical values for all j that are associated with any fixed i. For the covariance function $\gamma(t,t')$, we use the stationary Matérn (1960) family:

$$\gamma(t,t') = \omega^2\{2^{\phi-1}\Gamma(\phi)\}^{-1}(\kappa|t-t'|)^{\phi}K_{\phi}(\kappa|t-t'|), \tag{3}$$

where $\Gamma(\phi)$ is the complete gamma function, $\omega^2 > 0$ denotes the variance, $\phi > 0$ is a shape parameter, $\kappa > 0$ is a scale parameter and K_{ϕ} is a modified Bessel function of the second kind of order ϕ. The corresponding Gaussian process $W_i(t)$ is $\lceil\phi\rceil - 1$ times mean-square differentiable, where '$\lceil\cdot\rceil$' denotes the ceiling function. An alternative way of capturing non-linear behaviour of repeated measurements is to specify the random effects as regression splines or polynomials with stochastic coefficients (Fitzmaurice *et al.* (2011), chapter 19). We do not consider these approaches in this paper, since they appear to us less natural than the stochastic process approach and would require many more parameters to achieve the same flexibility in shape. That said, there are connections between an integrated random-walk process and a smoothing spline representation of the $W_i(t)$ (Wahba, 1990; Zhu and Dunson, 2017).

Likelihood-based inference for model (2) is straightforward. The likelihood function is a product of m multivariate normal densities with dimensions n_i. For typical study designs, the n_i are sufficiently small that the required matrix calculations are not computationally demanding.

In the continuous time setting, it is helpful to exploit an alternative representation of a Gaussian process $W(\cdot)$ as the solution to a stochastic differential equation,

$$\mathcal{D}W(t) = \mathrm{d}L(t), \tag{4}$$

where $\mathcal{D}$ is a differential operator and $\mathrm{d}L(t)$ is continuous time Gaussian white noise (Lindgren *et al.*, 2011). For example, the integrated random-walk model used by Diggle *et al.* (2015) and Zhu and Dunson (2017) corresponds to $\mathcal{D} = \partial^2/\partial t^2$, whereas the Matérn model corresponds to

$$\mathcal{D} = \left(\kappa^2 - \frac{\partial^2}{\partial t^2}\right)^{(2\phi+1)/4}. \tag{5}$$

For the stochastic differential equation representation of an integrated Ornstein–Uhlenbeck process, see Zhu *et al.* (2011a,b).

In applications for which only the regression parameters $\boldsymbol{\beta}$ are of scientific interest, estimating equations offer an alternative to likelihood-based estimation. In the current context, this approach was introduced by Liang and Zeger (1986), working in the wider setting of generalized linear models. For linear models, the approach consists of estimating $\boldsymbol{\beta}$ by weighted least squares; hence

$$\tilde{\boldsymbol{\beta}} = \left(\sum_{i=1}^{m} \mathbf{x}_i^{\mathrm{T}}\mathbf{F}_i\mathbf{x}_i\right)^{-1} \sum_{i=1}^{m} \mathbf{x}_i^{\mathrm{T}}\mathbf{F}_i\mathbf{Y}_i, \tag{6}$$

where, for each i, $\mathbf{Y}_i = (Y_{i1}, \ldots, Y_{in_i})^{\mathrm{T}}$, $\mathbf{x}_i$ is the $n_i \times k$ matrix whose jth row is $\mathbf{x}_{ij}^{\mathrm{T}}$ and the $\mathbf{F}_i$ are weight matrices. Rewriting equation (6) in an obvious shorthand notation as $\tilde{\boldsymbol{\beta}} = \mathbf{DY}$, inference for $\boldsymbol{\beta}$ uses the result that $\tilde{\boldsymbol{\beta}}$ is asymptotically multivariate Gaussian with mean $\boldsymbol{\beta}$ and variance $\mathbf{DCD}^{\mathrm{T}}$, where $\mathbf{C} = \mathrm{var}(\mathbf{Y})$, a block diagonal matrix with non-zero blocks, $\mathbf{C}_i = \mathrm{var}(\mathbf{Y}_i)$. If $\mathbf{F}_i = \mathbf{C}_i^{-1}$, then $\tilde{\boldsymbol{\beta}}$ is the maximum likelihood estimator for $\boldsymbol{\beta}$.

The basic idea behind equation (6) is to choose, rather than to estimate, a set of matrices $\mathbf{F}_i$ that reflect a reasonable *working covariance structure* for the matrices $\mathbf{C}_i = \mathrm{var}(\mathbf{Y}_i)$, but not to rely on the correctness of the chosen structure. Instead, the unknown matrix $\mathbf{C}_i$ is replaced by a non-parametric estimate $\tilde{\mathbf{C}}_i$. One such set of estimates is given by $\tilde{\mathbf{C}}_i = n_i^{-1}(\mathbf{Y}_i - \mathbf{x}_i\tilde{\boldsymbol{\beta}})(\mathbf{Y}_i - \mathbf{x}_i\tilde{\boldsymbol{\beta}})^{\mathrm{T}}$. Individually, each $\tilde{\mathbf{C}}_i$ is a very poor estimate of $\mathbf{C}_i$, but the implicit averaging in equation (6) leads to consistent estimation of $\mathrm{var}(\tilde{\boldsymbol{\beta}})$ in the limit $m \to \infty$ for fixed n_i (Liang and Zeger, 1986).

2.2. Non-Gaussian models for real-valued repeated measurement data

The existing literature on non-Gaussian models takes as its starting point a linear model with correlated errors:

$$Y_{ij} = \mathbf{x}_{ij}^{\mathrm{T}}\boldsymbol{\beta} + S_{ij}, \tag{7}$$

where, in the case of a common set of follow-up times, $t_1, \ldots, t_n$, for each subject, the $\mathbf{S}_i = (S_{i1}, \ldots, S_{in})^{\mathrm{T}}$ are independent copies of a zero-mean multivariate normal random vector (Jennrich and Schluchter, 1986). Most references consider the Laird–Ware approach as presented in model (1), where

$$S_{ij} = \mathbf{d}_{ij}^{\mathrm{T}}\mathbf{U}_i + Z_{ij}. \tag{8}$$

Liu and Rubin (1995), Lange *et al.* (1989) and Pinheiro *et al.* (2001) replaced each S_{ij} in equation (7) or (8) by $S_{ij}^* = S_{ij}/\sqrt{V_i}$, where the V_i are mutually independent unit mean gamma-distributed random variables. They estimated the model parameters by maximum likelihood using an expectation–maximization algorithm (Dempster *et al.*, 1977). Lin and Wang (2011) considered Bayesian methods of inference for the same class of models. Matos *et al.* (2013) extended the work of Pinheiro *et al.* (2001) to allow censored outcomes.

Song *et al.* (2007) and Zhang *et al.* (2009) considered an extension to Lange *et al.* (1989) by allowing the gamma-distributed scaling factor V_i to apply to either one of the two components on the right-hand side of equation (8). Lin and Lee (2007) applied the gamma-distributed scaling factor only to the random-effects term $\mathbf{d}_{ij}^{\mathrm{T}}\mathbf{U}_i$ but also replaced the mutually independent Z_{ij} by a set of auto-regressive processes; this restricts its applicability to data with equally spaced measurement times.

Rosa *et al.* (2003) and Tian *et al.* (2008) also used the formulation $S_{ij}^* = S_{ij}/\sqrt{V_i}$, but without restricting the V_i to be gamma distributed. Lange and Sinsheimer (1993) called the resulting family of distributions the *normal–independent* family, a special case of which is a mixture of normal distributions. The R package `heavy` (Osorio, 2016) fits this class of models. In a series of papers, V. H. Lachos and colleagues have developed methodology for fitting non-linear mixed models by using the normal–independent family; see Lachos *et al.* (2009, 2010, 2011, 2012, 2013) Zeller *et al.* (2010) and Cabral *et al.* (2012) and also independent contributions by Verbeke and Lesaffre (1996), Sun *et al.* (2008), Ho and Lin (2010), De la Cruz (2014), Zhang *et al.* (2015) and Yavuz and Arslan (2016).

Several researchers have extended the single-term modelling framework (8) by decoupling the scalings of the random effects and the measurement error terms. See, for example, Rosa *et al.* (2004), Aralleno-Valle *et al.* (2007), Jara *et al.* (2008), Meza *et al.* (2012), Choudhary *et al.* (2014) and Bai *et al.* (2016). Lu and Zhang (2014) extended the approach to include non-ignorable drop-out.

Wang and Fan (2011, 2012), Lin and Wang (2013) and Kazemi *et al.* (2013) used the normal–independent family to model multivariate repeated measurement data.

Others have taken a semiparametric approach to the problem, for example by using a Dirichlet process prior for the random effects or leaving the random-effects distribution unspecified. See Kleinman and Ibrahim (1998), Ghidey *et al.* (2004), Tao *et al.* (2004), Subtil and Rabilloud (2010), Davidian and Gallant (1993), Zhang and Davidian (2001) and Vock *et al.* (2012). Koller (2016) considered robust estimating equations.

We have found only two references that considered the general form of model (2) with three stochastic components with the single-term formulation (8), namely Stirrup *et al.* (2015) and Asar *et al.* (2016), and none that allows the three scaling factors to be decoupled.

3. A flexible class of non-Gaussian models

Our aim in this section is to set out a version of the mixed effects model

$$Y_{ij} = \mathbf{x}_{ij}^{\mathrm{T}}\beta + \mathbf{d}_{ij}^{\mathrm{T}}\mathbf{U}_i + W_i(t_{ij}) + \sigma Z_{ij}, \qquad j = 1, \dots, n_i, \quad i = 1, \dots, m, \tag{9}$$

that, we believe for the first time, allows Gaussian or non-Gaussian distributional specifications of the three stochastic components $\mathbf{U}_i$, $W_i(t)$ and Z_{ij} to be decoupled.

Writing $\mathbf{B}$ and $\mathbf{H}$ to denote generic vector-valued random variables, we replace the Gaussian assumption for each of the components with a normal variance–mean mixture of the form

$$\mathbf{B} = \boldsymbol{\delta} + \boldsymbol{\mu} V + \sqrt{V}\boldsymbol{\Sigma}^{1/2}\mathbf{H}, \tag{10}$$

where $\boldsymbol{\delta}$ and $\boldsymbol{\mu}$ are parameter matrices, $\mathbf{H} \sim N(\mathbf{0}, \mathbf{I})$ with $\mathbf{I}$ being the identity, and V is a random variable that takes values on $\mathbb{R}^+$. We need to impose some restrictions on the distribution of V for the inferential algorithms that we develop in Section 4 to be practicable. For the subject-specific *random effect* $\mathbf{U}_i$ and the measurement-specific *noise* Z_{ij} the only necessary restriction is that V has a known distribution. However, to simplify parameter estimation, we shall impose the additional restriction that $V|\mathbf{H}$ also has a known distribution. For the subject-specific continuous time *stochastic process* $W_i(t)$ we use a numerical discretization of the differential operator (4) to generate realizations of the process. For this reason, we need the distribution to be closed under arbitrary discretization, which we ensure by requiring that the distribution of V be closed under convolution. Our specific proposals for $\mathbf{U}_i$, $W_i(t)$ and Z_{ij} are described below in more detail.

A flexible choice for $\mathbf{B}$ is the multivariate generalized hyperbolic (GH) distribution (Barndorff-Nielsen, 1977; Vilca *et al.*, 2014). This distribution can be generated from the mixture representation (10) by specifying a generalized inverse Gaussian (GIG) distribution for V. The density function of the GIG distribution is

$$f(x; p, a, b) = \frac{(a/b)^{p/2}}{2K_p(\sqrt{ab})} x^{p-1} \exp\left(-\frac{a}{2}x - \frac{b}{2}x^{-1}\right), \tag{11}$$

where K_p is the modified Bessel function of the third kind, of order p, whereas a and b are positive-valued parameters. We denote this distribution by $\mathrm{GIG}(p, a, b)$ and refer the reader to Jørgensen (1982) for more details. An important property of this distribution is that, for any $c > 0, cV \sim \mathrm{GIG}(p, a/c, cb)$. Another property that is useful for the construction of the sampling-based inferential algorithms that we introduce in Sections 4.2 and 4.4 is that the conditional distribution of V given the observed data is also GIG.

The GH distribution includes several widely used distributions as special cases, e.g. the Student t, generalized asymmetric Laplace (GAL), normal–inverse Gaussian (NIG) and Cauchy distributions. Specific parameter configurations for the distributions of V that give each of these special cases are presented in Table 1. Note that, for both the NIG and the GAL distributions, the formulation is overparameterized for $\mathbf{B}$ in equation (10). One therefore needs to fix a or b.

3.1. Noise and random effects

Since the measurement noise is univariate, we can write the mixture representation (10) as

$$Z_{ij} = \delta^Z + \mu^Z V_{ij}^Z + \sigma\sqrt{V_{ij}^Z} Z_{ij}^*, \tag{12}$$

where $Z_{ij}^* \sim N(0, 1)$. To maintain the interpretation of σ^2 as the variance of the noise, at least in the symmetric case, we constrain the values of the GIG parameters a, b and p, so that $E[V_{ij}^Z] = 1$,

Table 1. Some special cases of the GH distribution, their mixing distributions and their corresponding GIG forms†

Distribution of $\mathbf{B}$	*Mixing distribution of* V	*GIG form of the mixing distribution*
t	$\mathrm{IGam}(\nu/2, \nu/2)$	$\mathrm{GIG}(\nu/2, \nu, 0)$
NIG	$\mathrm{IG}(a, b)$	$\mathrm{GIG}(-\frac{1}{2}, a, b)$
GAL	$\mathrm{Gam}(p, a)$	$\mathrm{GIG}(p, 2a, 0)$
Cauchy	$\mathrm{IGam}(\frac{1}{2}, b/2)$	$\mathrm{GIG}(-\frac{1}{2}, 0, b)$

†Gam indicates the gamma family of distributions, IGam the inverse gamma family and IG the inverse Gaussian family.

and hence $\mathrm{var}(\sigma\sqrt{V_{ij}^Z} Z_{ij}^*) = \sigma^2$. We further set $\delta^Z = -\mu^Z$ to ensure that the measurement noise is zero mean, i.e. $E[Z_{ij}] = 0$.

An alternative to representation (12) is to attach a single random variable V_i^Z to all of the noise terms Z_{ij} on the ith subject, i.e. $Z_{ij} = \delta^Z + \mu^Z V_i^Z + \sqrt{V_i^Z} \sigma Z_{ij}^*$. The distribution of V_i can then be interpreted as a random effect for patient-specific measurement noise variance. Note, in particular, that this introduces stochastic dependence between Z_{ij} and $Z_{ij'}$ for $j \neq j'$, although they are conditionally independent given V_i^Z.

For the random effects, we let $\mathbf{U}_i = \boldsymbol{\delta}^U + \boldsymbol{\mu}^U V_i^U + \sqrt{V_i^U} \Sigma^{1/2} \mathbf{U}_i^*$, where V_i is a unit-mean GIG random variable and $\mathbf{U}_i^* \sim N(\mathbf{0}, \mathbf{I})$ with $\mathbf{I}$ as before. We again set $\boldsymbol{\delta}^U = -\boldsymbol{\mu}^U$ to ensure that $E[\mathbf{U}_i] = \mathbf{0}$.

3.2. *Stochastic process*

A simple way to introduce a non-Gaussian stochastic process term in expression (9) would be again to include a subject-specific scaling, i.e. $W_i(t) = V_i^W W_i^*(t)$, where V_i^W follows a unit mean GIG distribution. However, this approach would not be able to capture interesting within-subject departures from Gaussian behaviour, e.g. jumps or asymmetries in the sample paths of $W_i(t)$. To provide the required flexibility, we instead use non-Gaussian generalizations of the stochastic differential equation (4). Specifically, we propose modelling the $W_i(t)$ as independent copies of the solution to

$$\mathcal{D} W_i(t) = \mathrm{d}L_i(t), \tag{13}$$

where the L_i are independent copies of a non-Gaussian Lévy process, i.e. a process with independent and stationary increments. In practice, we work with a discretized version of equation (13), for which Bolin (2014) showed that a type G Lévy process for $L_i(t)$ is a suitable candidate. The implication is that the increments of L_i have a distribution that corresponds to the specification given by equation (10).

One approach would therefore be to choose the distribution of V^W as a GIG distribution, which would yield the GH processes of Eberlein (2001). However, as noted earlier, we require the distribution of V^W to be closed under convolution (Wallin and Bolin, 2015). Also, the stochastic gradient method for parameter estimation that we introduce in Section 4 requires the ability to sample from the conditional distribution of V^W given all other components in the model. Within the GH family, the NIG, GAL and Cauchy distributions are the only ones that meet these requirements (Podgórski and Wallin, 2016). In Table 2, we present the parameterization of the mixing distribution for the three cases. Using any of these distributions for the increments of L_i

Table 2. The parameterizations of the three types of GH processes satisfying closure under convolution

Distribution of $L(t)$	*Mixing distribution of V^W*	*GIG form of the mixing distribution*
Cauchy	$\mathrm{IGam}(\frac{1}{2}, t^2/2)$	$\mathrm{GIG}(-\frac{1}{2}, 0, t^2)$
NIG	$\mathrm{IG}(a, bt^2)$	$\mathrm{GIG}(-\frac{1}{2}, a, bt^2)$
GAL	$\mathrm{Gam}(pt, a/2)$	$\mathrm{GIG}(pt, a, 0)$

in equation (13) results in models with the same covariance structure as if L_i were Gaussian, but with more general marginal distributions. The NIG choice makes L_i an NIG process (Barndorff-Nielsen, 1997a). This class of processes has been used in financial modelling; see Barndorff-Nielsen (1997b), Bibby and Sørensen (2003), Tankov (2003) and Eberlein (2001), for more details.

3.2.1. The choice of operator

As previously mentioned, using $\mathcal{D}$ as in equation (5) yields a process with a Matérn covariance function. More specifically, if the process is defined on the entire real line, then it has Matérn covariance. In practice, we restrict the process to a bounded temporal interval and impose boundary conditions on the operator to obtain a well-posed problem. Common choices for these artificial boundary conditions are either homogeneous Neumann or homogeneous Dirichlet conditions. The effect of these artificial boundary conditions is small for distances that are larger than twice the practical correlation range of the process (Lindgren *et al.*, 2011). We therefore define the process on an extended temporal domain $\tilde{T} = [-r, t_{\max} + r]$ where all measurement times lie within the interval $[0, t_{\max}]$ and r is a value that is larger than the practical correlation range.

For $\phi = \frac{1}{2}$, the operator (5) is $\mathcal{D}_1 = (\kappa^2 - \partial^2/\partial t^2)^{1/2}$, which results in a process with an exponential covariance function $E[W(t)W(t+h)] = (2\kappa)^{-1}\exp(-\kappa|h|)$. Another, perhaps more natural, choice that results in a process with exponential covariance when defined on the entire real line is $\mathcal{D}_2 = \kappa + \partial/\partial t$. This can easily be seen by computing the power spectrum $S_W(\omega)$ of the corresponding stochastic process. Taking the Fourier transform of the stochastic differential equation gives $(\kappa + \mathrm{i}\omega)\hat{W}(\omega) = \widehat{\mathrm{d}L}(\omega)$. Using the fact that the power spectrum of $\widehat{\mathrm{d}L}(\omega)$, is constant, it follows that

$$S_W(\omega) \propto \{(\kappa + \mathrm{i}\omega)(\kappa - \mathrm{i}\omega)\}^{-1} = (\kappa^2 + \omega^2)^{-1},$$

which we recognize as the spectral density corresponding to the exponential covariance function. This result is well known, since in the Gaussian case the process is the classical Ornstein–Uhlenbeck process. When posed on the bounded domain T, we only have to equip $\mathcal{D}_2$ with one boundary condition. A natural choice in this case is a stochastic Dirichlet boundary condition at either end point of T, $W(0) = W$ or $W(T) = W$, where W is a random variable with distribution equal to the marginal distribution for $W(t)$, when the model is formulated on the entire real line. This results in a stationary model and there is no need to extend the domain of interest.

When the driving noise of the process is Gaussian, the models that are formulated by using $\mathcal{D}_1$ and $\mathcal{D}_2$ are equivalent in distribution (apart from the behaviour at the boundary of the domain). However, for non-Gausisan models the processes that are formulated by using the two choices are *not* equivalent: the kernel of $\mathcal{D}_1$ is symmetric, whereas the kernel of $\mathcal{D}_2$ is completely asymmetric. This affects the appearance of trajectories of the process. For $\mathcal{D}_1$, the trajectories are symmetric in time, i.e. the process is time reversible, whereas the trajectories can be asymmetric when $\mathcal{D}_2$ is used. The difference between the symmetric and asymmetric models is illustrated in Fig. 2, where the same driving NIG noise is used to simulate a trajectory using $\mathcal{D}_1$ and $\mathcal{D}_2$. Using $\mathcal{D}_2$ allows for sharp jumps in the trajectories that are not present when $\mathcal{D}_1$ is used.

One way to construct a model with a general Matérn covariance that allows for asymmetries in the sample paths is to add a fractional exponent to $\mathcal{D}_2$, to give $\mathcal{D}_3 = (\kappa + \partial/\partial t)^{(2\phi+1)/2}$. This results in a process with a Matérn covariance, but with asymmetry in the trajectories depending on where boundary conditions are imposed. It should be noted that these models have Markov properties when $\phi = \frac{1}{2}, \frac{3}{2}, \frac{5}{2}, \ldots$, which simplifies simulation as explained in the next section.

Besides the Matérn models, another option that is used for longitudinal data is the integrated random-walk model (Diggle *et al.*, 2015). This can be seen as a special case of $\mathcal{D}_3$ with $\kappa = 0$ and $\phi = \frac{3}{2}$, and can thus be handled in the same way as the Matérn models.

3.2.2. Discretization

We need to discretize time to use the stochastic differential equation (13). For this, we use the approximation

$$W(t) = \sum_{k=1}^{K} \phi_k(t) W_k, \tag{14}$$

where $\mathbf{W} = (W_1, \ldots, W_K)^{\mathrm{T}}$ is a vector of random variables and the $\phi_k(t)$ are basis functions. We use a set of piecewise linear basis functions such that

$$\phi_1(t) = \begin{cases} 1 - \dfrac{t - s_1}{s_2 - s_1}, & s_1 < t < s_2, \\ 0, & \text{otherwise}, \end{cases}$$
$$\phi_K(t) = \begin{cases} \dfrac{t - s_{k-1}}{s_k - s_{k-1}}, & s_{k-1} < t < s_k, \\ 0, & \text{otherwise}, \end{cases}$$

and, for $k = 2, 3, \ldots, (K-1)$,

$$\phi_k(t) = \begin{cases} \dfrac{t - s_{k-1}}{s_k - s_{k-1}}, & s_{k-1} < t < s_k, \\ 1 - \dfrac{t - s_k}{s_{k+1} - s_k}, & s_k < t < s_{k+1}, \\ 0, & \text{otherwise}, \end{cases}$$

where $0 = s_1 < s_2 < \ldots < s_{K-1} < s_K = t_{\max}$. In the case of a Dirichlet boundary condition at $t = 0$, the function ϕ_1 is removed from the expansion, whereas, in the case of the Dirichlet boundary condition at $t = t_{\max}$, ϕ_K is removed. The distribution of the stochastic weights is computed by using either a Galerkin finite element discretization or a Petrov–Galerkin method depending on the operator; details are given in Appendix B. The result for the non-Gaussian case can be written as

$$\mathbf{W}|\mathbf{V}^{\mathbf{W}} \sim N[\mathbf{K}^{-1}\{\mathbf{h}^{\mathrm{T}}\delta^{W} + (\mathbf{V}^{\mathbf{W}})^{\mathrm{T}}\mu^{W}\}, \mathbf{K}^{-1}\,\mathrm{diag}(\mathbf{V}^{\mathbf{W}})(\mathbf{K}^{-1})^{\mathrm{T}}], \tag{15}$$

where $\mathbf{K}$ is a matrix corresponding to a discretization of the differential operator and $V_k^W \sim \mathrm{IG}(\nu, h_k^2\nu)$ where h_k are fixed constants depending on the basis functions. Note that we again set $\delta^W = -\mu^W$ to satisfy $E[W(t)] = 0$.

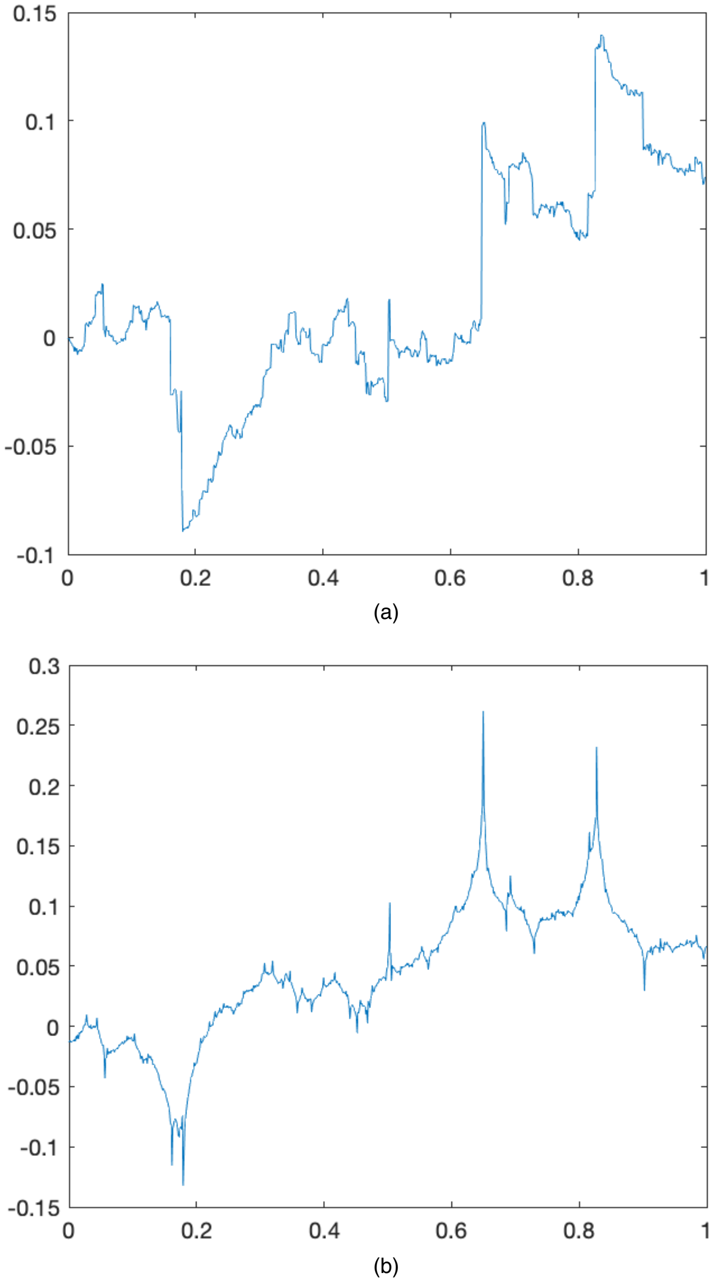

(a)

(b)

Fig. 2. Simulation of an NIG process with exponential covariance function using the operator (a) $\mathcal{D}_2$ and (b) $\mathcal{D}_1$, with the same driving noise in both cases: one can note that the trajectory is asymmetric in (a)

Note that the parameter ν controls the tails of the marginal distribution of the process. The limiting case $\nu \to 0$ is the Cauchy process, whereas the limiting case $\nu \to \infty$ is a Gaussian process. These are exactly the properties that we need to use our likelihood-based methods to assess whether a standard, and undeniably convenient, Gaussian assumption for any or all of the stochastic components of expression (9) is adequate.

4. Likelihood-based inference

4.1. Hierarchical representation

Our specification of a normal variance–mean mixture for each of the stochastic components of expression (9) makes likelihood-based inference practicable via the following hierarchical representation of the model. For subject i, let $\mathbf{V}_i^Z$, V_i^U and $\mathbf{V}_i^W$ denote the stochastic variance factors corresponding to the noise, random-effects and stochastic process components of expression (9), and write $\mathbf{Y}_i = (Y_{i1}, \ldots, Y_{in_i})^{\mathrm{T}}$ for the corresponding set of repeated measurements. Let $\mathbf{W}_i = \{W_{ik} : k = 1, \ldots, K\}$ be the stochastic weight vector for the ith subject in the approximation of $W_i(t)$ given by equation (14), and $\mathbf{A}_i$ the $n_i \times K$ matrix with (j, k)th element $\phi_k(t_{ij})$. Write $\mathbf{x}_i$ and $\mathbf{d}_i$ for the matrices with jth rows $\mathbf{x}_{ij}^{\mathrm{T}}$ and $\mathbf{d}_{ij}^{\mathrm{T}}$ respectively. Finally, let $\boldsymbol{\Theta}$ denote the complete set of model parameters. The model for the ith subject then has the following hierarchical representation:

$$\mathbf{Y}_i | \mathbf{W}_i, \mathbf{U}_i, \mathbf{V}_i^Z \sim N\{\mathbf{x}_i^{\mathrm{T}} \boldsymbol{\beta} + \mathbf{d}_i^{\mathrm{T}} \mathbf{U}_i + \mathbf{A}_i \mathbf{W}_i + (-1 + \mathbf{V}_{\mathbf{i}}^{\mathbf{Z}}) \mu^z, \sigma^2 \operatorname{diag}(\mathbf{V}_i^Z)\},$$

$$\mathbf{U}_i | V_i^U \sim N(-\boldsymbol{\mu}^U + \boldsymbol{\mu}^U V_i^U, V_i^U \boldsymbol{\Sigma}),$$

$$\mathbf{W}_i | \mathbf{V}_i^W \sim N\{\mathbf{K}^{-1}(-\mu^W \mathbf{h} + \mu^W \mathbf{V}_i^W), \mathbf{K}^{-1} \operatorname{diag}(\mathbf{V}_i^W)(\mathbf{K}^{-1})^{\mathrm{T}}\},$$

coupled with a final layer in the hierarchy: the distributions of the stochastic variance factors. The distributions are GIG distributed with parameters that depend on the model choice. Integrating out the latent variables and variance components, these equations collectively determine the contribution of the ith subject to the marginal log-likelihood $L(\boldsymbol{\Theta}; \mathbf{Y}_i)$. As the vectors $\mathbf{Y}_i$ from the m subjects are independent, the overall log-likelihood is

$$L(\boldsymbol{\Theta}; \mathbf{Y}) = \sum_{i=1}^{m} L_i(\boldsymbol{\Theta}; \mathbf{Y}_i).$$

4.2. Stochastic gradient estimation

The computations that are required for maximum likelihood estimation are cumbersome for problems that involve longitudinal data sets with large numbers of subjects and repeats, even using the computationally efficient approximation (14). Our proposed algorithm for maximum likelihood estimation therefore uses a stochastic gradient method that calculates the gradient of the objective function at each step of the maximization by subsampling.

A stochastic gradient method for the general problem of minimizing an objective function $f(\boldsymbol{\Theta})$ starts with an initial guess $\boldsymbol{\Theta}^{(0)}$, and then iteratively updates $\boldsymbol{\Theta}$ according to

$$\boldsymbol{\Theta}^{(n+1)} = \boldsymbol{\Theta}^{(n)} + \eta_n Q_n(\boldsymbol{\Theta}^{(n)}), \tag{16}$$

where $Q_n(\boldsymbol{\Theta})$ is a random variable such that $E[Q_n(\boldsymbol{\Theta})] = \nabla_{\boldsymbol{\Theta}} f(\boldsymbol{\Theta})$ and η_n is a sequence of positive numbers such that $\Sigma_{n=1}^{\infty} \eta_n = \infty$ and $\Sigma_{n=1}^{\infty} \eta_n^2 < \infty$; an example is $\eta_n \propto 1/\eta^n$ with $0.5 < \eta \leqslant 1$. Under mild regularity conditions, the resulting sequence $\boldsymbol{\Theta}^{(n)}$ converges to a stationary point of $f(\boldsymbol{\Theta})$ (Kushner and Yin, 2003; Andrieu *et al.*, 2007).

For maximum likelihood estimation, $f(\boldsymbol{\Theta}) = -L(\boldsymbol{\Theta}; \mathbf{Y})$. If the data set contains a large number of subjects we use only a small, randomly sampled subset in each iteration to generate a computationally efficient stochastic gradient method. For this, $\nabla_{\boldsymbol{\Theta}} L(\boldsymbol{\Theta}; \mathbf{Y})$ can be replaced by the random variable

$$Q_n(\boldsymbol{\Theta}) = \nabla_{\boldsymbol{\Theta}} L_s(\boldsymbol{\Theta}; \mathbf{Y}) = s \sum_{i=1}^{m} \nabla_{\boldsymbol{\Theta}} L_i(\boldsymbol{\Theta}; \mathbf{Y}_i) J_i, \tag{17}$$

where the J_i are independent Bernoulli random variables with $P(J_i=1)=1/s$. Since the expected value of $\nabla_{\Theta} L_s(\Theta;\mathbf{Y})$ with respect to these random variables is equal to $\nabla_{\Theta} L(\Theta;\mathbf{Y})$ for any s, the resulting stochastic gradient method (16) will converge to a stationary point of the log-likelihood. Our experience, for example with the two case-studies that we describe in Section 6, has been that, for data sets containing a large number of subjects, often we need only a small proportion of the available measurement sequences $\mathbf{Y}_i$ at each iteration to estimate the parameters reliably. For example, we used only 688 (3%) subjects out of 22910 for the renal case-study that is presented in Section 6.2.

For our non-Gaussian models, an additional complication is that the likelihood is not available in an explicit form. However, using Fisher's identity (Dempster *et al.*, 1977) we can compute the gradient of the log-likelihood without computing the log-likelihood itself. For all versions of our model, the log-likelihood conditional on the variance components $\mathbf{V}=\{\mathbf{V}_i^W,\mathbf{V}_i^U,\mathbf{V}_i^Z\}_{i=1}^m$ is Gaussian and thus explicit. Fisher's identity then gives

$$\nabla_{\Theta} L_s(\Theta;\mathbf{Y}) = E_{\mathbf{V}}\{\nabla_{\Theta} L_s(\Theta;\mathbf{Y},\mathbf{V})|\mathbf{Y}\},$$

where $L_s(\Theta;\mathbf{Y},\mathbf{V})$ is the log-likelihood augmented with $\mathbf{V}$, which is explicitly available since $\mathbf{Y}|\mathbf{V}$ is Gaussian and $\mathbf{V}$ is GIG. The expectation with respect to $\mathbf{V}$ is not, in general, explicit but can be approximated by Monte Carlo (MC) sampling from the conditional distribution $\mathbf{V}|\mathbf{Y}$. We use a Gibbs sampler and iterate between sampling from the conditional distributions $\mathbf{V}|\mathbf{U}, \mathbf{W}, \mathbf{Y}$ and $\mathbf{U}, \mathbf{W}|\mathbf{V}, \mathbf{Y}$, where $\mathbf{U}=\{\mathbf{U}_i\}_{i=1}^m$ and $\mathbf{W}=\{\mathbf{W}_i\}_{i=1}^m$; for details, see Appendix A. Convergence of algorithms of this kind was studied in Andrieu *et al.* (2007).

When using stochastic gradient optimization to maximize over many parameters, it is important to scale the gradient by a preconditioner to give a Newton-like iteration. Our proposed algorithm therefore is

$$\Theta^{(n+1)} = \Theta^{(n)} + \eta_n \mathbf{I}(\Theta^{(n)})^{-1} Q_n(\Theta^{(n)}), \tag{18}$$

where $\mathbf{I}(\Theta^{(n)})^{-1}$ is a preconditioner to be determined and $Q_n(\Theta^{(n)})$ is a stochastic approximation of the gradient based on subsampling and MC integration over $\mathbf{V}$ using the Gibbs sampler. One option for the preconditioner is $\mathbf{I}^*(\Theta) = -E_{\mathbf{V}}[\nabla^2_{\Theta} L_s(\Theta;\mathbf{Y},\mathbf{V})|\mathrm{Y}]$. Calculation of $\mathbf{I}^*(\Theta)$ is typically easy, since $\nabla^2_{\Theta} L_s(\Theta;\mathbf{Y},\mathbf{V})$ is often explicit and can be calculated simultaneously with the gradient. Lange (1995) described the connection between using $\mathbf{I}^*(\Theta)$ and the expectation–maximization algorithm. However, if the same variables are used for the MC estimates of the expectations in $\mathbf{I}^*(\Theta)$ and $Q_n(\Theta)$, the joint updating step (18) will be biased because of correlation between the two estimated expectations. One way to avoid this is to use different samples of $\mathbf{V}|\mathbf{Y}$ to compute the two expectations. Instead we use a preconditioner that is similar to the *complete* Fisher information cFIM,

$$\mathbf{I}_{\mathrm{cFIM}}(\Theta) = -E_{\mathbf{V},\mathbf{Y}}[\nabla^2_{\Theta} L_s(\Theta;\mathbf{Y},\mathbf{V})], \tag{19}$$

which often can be computed explicitly. Note that, in equation (19), the expectation is taken over both $\mathbf{Y}$ and $\mathbf{V}$. Since the expectation is not conditioned on $\mathbf{Y}$, cFIM does not suffer from the same biasedness issues as $\mathbf{I}^*(\Theta)$. However, it can still be biased if subsampling is used, and we therefore use a preconditioner that is a weighted average of $\mathbf{I}_{\mathrm{cFIM}}(\Theta)$ over past iterations to reduce the bias. The use of cFIM is not ideal because it may result in slow convergence, but it is the best available option. The *standard* Fisher information matrix, $\mathbf{I}_{\mathrm{FIM}}(\Theta) = -E_{\mathbf{Y}}[\nabla^2_{\Theta} L_{\mathrm{s}}(\Theta;\mathbf{Y})]$, is seldom explicit and thus cannot be used as a preconditioner. However, we do need to estimate either the standard or the *observed* Fisher information matrix oFIM, $\mathbf{I}_{\mathrm{oFIM}}(\Theta) = -\nabla^2_{\Theta} L_{\mathrm{s}}(\Theta;\mathbf{Y})$, to calculate confidence intervals for the estimated parameters. We estimate $\mathbf{I}_{\mathrm{oFIM}}(\Theta)$ by using

Louis's identity (Louis, 1982),

$$\mathbf{I}_{\mathrm{oFIM}}(\mathbf{\Theta}) = -E_{\mathbf{V}}[\nabla^2_{\mathbf{\Theta}} L_{\mathrm{s}}(\mathbf{\Theta}; \mathbf{Y}, \mathbf{V})|\mathbf{Y}] - \mathrm{var}_{\mathbf{V}}\{\nabla_{\mathbf{\Theta}} L_{\mathrm{s}}(\mathbf{\Theta}; \mathbf{Y}, \mathbf{V}) \nabla_{\mathbf{\Theta}} L_{\mathrm{s}}(\mathbf{\Theta}; \mathbf{Y}, \mathbf{V})^{\mathrm{T}}|\mathbf{Y}\}. \qquad (20)$$

Both terms on the right-hand side of equation (20) can be estimated by MC sampling, as proposed for $\nabla_{\mathbf{\Theta}} L_{\mathrm{s}}(\mathbf{\Theta}; \mathbf{Y})$ in equation (17). We could also estimate $\mathbf{I}_{\mathrm{FIM}}(\mathbf{\Theta})$ by an additional sampling step, using the fact that $\mathbf{I}_{\mathrm{FIM}}(\mathbf{\Theta}) = E_{\mathbf{Y}}[\mathbf{I}_{\mathrm{oFIM}}(\mathbf{\Theta})]$. For more details on the calculation of the gradients required and oFIM, see Appendix A.

4.3. Multiple-chain estimation

A drawback of the estimation procedure that was described in the previous subsection is that the stochastic nature of the method can make it difficult to determine a suitable stopping criterion. To overcome this problem, we propose running several independent estimation procedures in parallel, starting from the same initial guess, i.e., using algorithm (18), we compute N_r different estimates of $\mathbf{\Theta}^{(n)}$, $\{\mathbf{\Theta}_i^{(n)} : i = 1, \ldots, N_r\}$, in parallel started from the same initial guess and using independent stochastic estimates of the gradient and preconditioner.

We combine these estimates by taking the mean of the N_r-estimates and calculate the estimate of the corresponding MC standard deviations $\boldsymbol{\sigma}^{(n)}$. These statistics are calculated, for the jth parameter, as

$$\Theta_j^{(n)} = \frac{1}{N_r} \sum_{i=1}^{N_r} \Theta_{i,j}^{(n)},$$

and

$$\boldsymbol{\sigma}^{(n)} = \left\{ \frac{1}{N_r} \sum_{i=1}^{N_r} (\Theta_{i,j}^{(n)} - \Theta_j^{(n)})^2 \right\}^{1/2},$$

where $\Theta_{i,j}^{(n)}$ denotes the jth element in $\mathbf{\Theta}_i^{(n)}$. We run each chain in batches. Whenever $n = kN_b$, for $k = 4, 5, 6, \ldots$ being the number of batches and N_b a chosen batch size (we use 1000 as default), we check whether each parameter Θ_j, the jth element of $\mathbf{\Theta}$, has converged on the basis of two criteria. The first is that $\sigma_j^{(n)} / \Theta_j^{(n)}$ should be smaller than a threshold, e.g. 0.1. This means that the MC variance should be sufficiently small for each parameter. The second convergence criterion is that the rate of change for each parameter should be sufficiently small. To check this, we estimate the intercept and slope of a simple linear regression model fit to the last four batch estimates of Θ_j (i.e. the values $\Theta_j^{((k-l)N_b)}$ for $l = 0, \ldots, 3$) as the outcome and iteration as the input. We then check whether the magnitude of the slope is not significantly larger than some constant (such as 0.01) times the magnitude of the intercept. We conclude convergence of a parameter if both criteria are satisfied and stop the estimation procedure if all parameters converge. An example of the trajectories for the multiple-chain estimation procedure is shown in Fig. 3.

The use of multiple chains has extra advantages, in addition to providing stopping criteria. The first is that the combined estimates that are based on multiple chains naturally have lower MC variances than the estimates that are based on using a single chain. The second is that the estimates of the MC variances can be used when computing confidence intervals for the parameters, which can improve coverages of Wald-type confidence intervals. Specifically, to compute a confidence interval for Θ_j, we use $\Theta_j \pm z_{\alpha/2} \surd\{(\sigma_j^{(n)})^2 + \sigma_j^2\}$, where $\sigma_j^{(n)}$ is the estimate of the MC standard deviation for the final iteration n, and σ_j^2 denotes the jth diagonal element of the inverse observed Fisher information matrix. Details on the calculation of the Fisher information matrix are given in Appendix A.

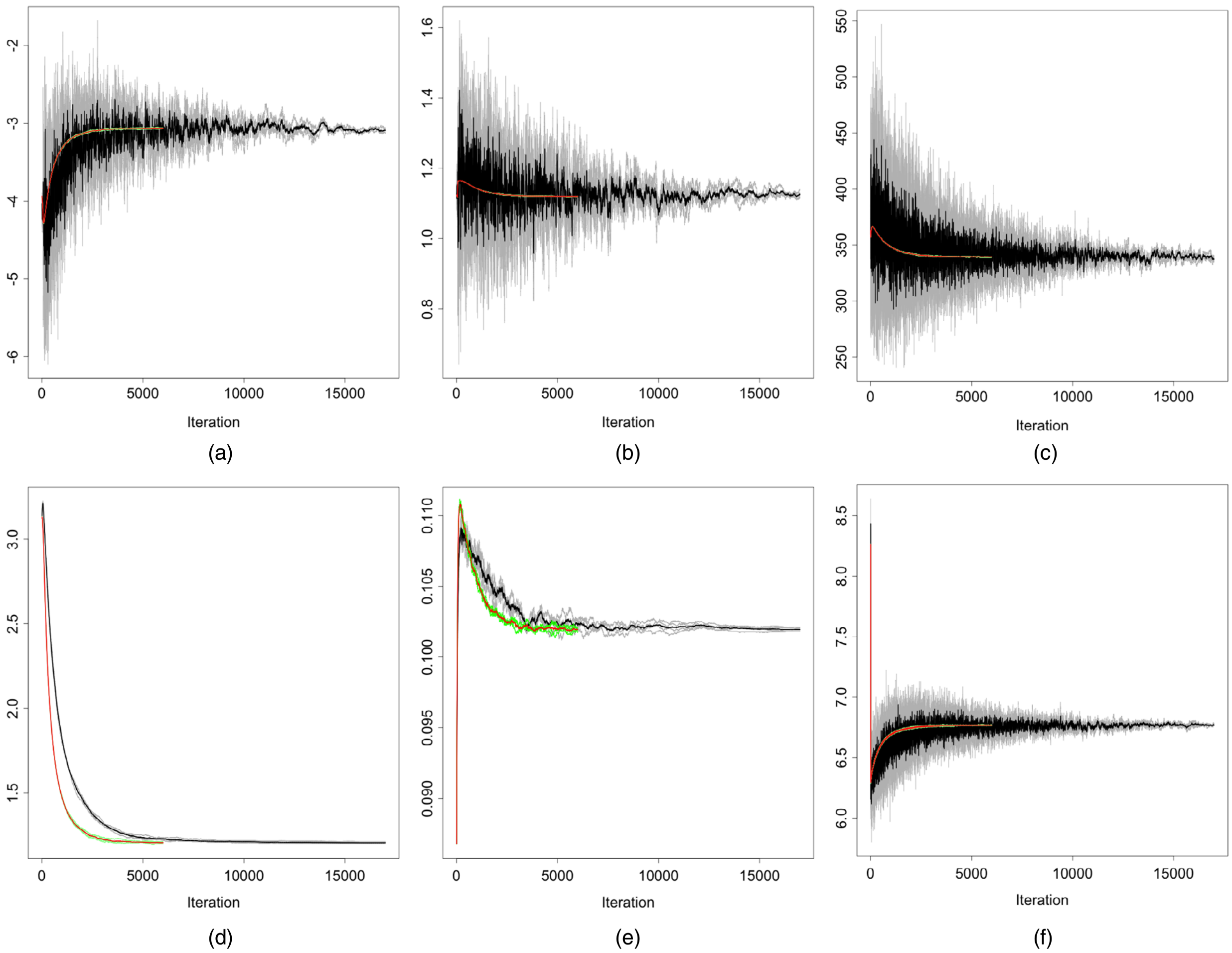

Fig. 3. Stochastic gradient estimation paths for results without subsampling (——) and with subsampling 20% of the patients in each iteration (——) (——, ——, the four individual paths that are run in parallel to compute these curves for results with and without subsampling; the automatic stopping criterion caused the estimation without subsampling to terminate after 6000 iterations whereas 17000 iterations were used with subsampling): (a) fixed effect; (b) fixed effect; (c) random effect Σ; (d) operator κ; (e) operator τ; (f) noise σ

4.4. Subsampling with fixed effects: the grouped subsampler

Another issue with the subsampling method that was described in Section 4.2 is that the subsampled matrices of covariates, $\mathbf{x}_i$, may not be of full rank. If this is so, none of the preconditioners that were described above can be used. In contrast, regular subsampling without any preconditioners may result in large MC variation in the estimated gradient. The cystic fibrosis case-study that we shall describe in Section 6.1 provides an example. These data are stratified into birth cohorts whose effects are important, but one of the cohorts contains only seven patients. This issue is related to subsampling for S-estimation algorithms in linear regression models (Koller and Stahel, 2016), but we could not find a satisfactory solution in the literature that could be applied in the current context. To address the issue, we therefore introduce the following subsampling procedure, which we call the *grouped subsampler*. The procedure first builds $k+1$ groups of subjects, $\mathcal{G}_0, \mathcal{G}_1, \ldots, \mathcal{G}_k$, in such a way that the matrices $\mathbf{x}_{\mathcal{G}_j} = \Sigma_{i \in \mathcal{G}_j} \mathbf{x}_i \mathbf{x}_i^{\mathrm{T}}$ have full rank for $j \geqslant 1$.

The groups are built iteratively starting with $\mathcal{G}_1$. To this group the first subject is added and one checks whether the covariate matrix $\mathbf{x}_{\mathcal{G}_1} = \mathbf{x}_1 \mathbf{x}_1^{\mathrm{T}}$ has full rank. If this is so, the formation of $\mathcal{G}_1$ is complete. Otherwise more subjects need to be added to the group. If $\mathbf{x}_{\mathcal{G}_1} + \mathbf{x}_2 \mathbf{x}_2^{\mathrm{T}}$ has a larger rank than $\mathbf{x}_{\mathcal{G}_1}$, the second subject is added to the group and $\mathbf{x}_{\mathcal{G}_1}$ is updated to $\mathbf{x}_{\mathcal{G}_1} + \mathbf{x}_2 \mathbf{x}_2^{\mathrm{T}}$. At this stage, the formation of $\mathcal{G}_1$ is complete if $\mathbf{x}_{\mathcal{G}_1}$ has full column rank; otherwise the procedure continues by adding more subjects in order until $\mathbf{x}_{\mathcal{G}_1}$ has full rank or until no further subjects are left. If the formation of $\mathcal{G}_1$ terminates because of a lack of further subjects, one cannot estimate the model on the basis of the available subjects. Otherwise, further groups $\mathcal{G}_2, \mathcal{G}_3, \ldots$ are constructed iteratively in the same way: subjects, who are not in any of the previous groups, are added to the group $\mathcal{G}_k$ until the covariate matrix $\mathbf{x}_{\mathcal{G}_k}$ has full rank. At some point, the group formation will terminate because of the lack of further subjects. If this happens during the formation of a group $\mathcal{G}_k$, this group is removed since its covariate matrix does not have full rank. Finally, any subjects who has not been assigned to a group are placed in the group $\mathcal{G}_0$. The procedure for forming the groups is described in pseudocode in algorithm 1 in Appendix A.4.

The groups are created as an initial stage before the estimation procedure begins. During the estimation procedure a subsampling step is performed as follows. Assume that we want to sample a proportion $p \in (0, 1)$ of the subjects. Let n_g be the total number of subjects in the groups $\mathcal{G}_0, \ldots, \mathcal{G}_k$. To ensure that we obtain a sample for which the subsampled covariate matrix has full column rank, we need to sample all subjects from at least one of the groups $\mathcal{G}_1, \ldots, \mathcal{G}_k$. Given this restriction, we would like to sample approximately pn_g subjects from the groups $\mathcal{G}_1, \ldots, \mathcal{G}_k$ as well as pn_0 subjects from $\mathcal{G}_0$. To do so, we first sample all the subjects from $m_g = \lceil pk \rceil$ out of the groups $\mathcal{G}_1, \ldots, \mathcal{G}_k$ chosen at random; then we sample $m_0 = \min\{\max([pN - Mk/n_g], 1), n_0\}$ subjects at random from $\mathcal{G}_0$; here, '$[\cdot]$' denotes the function that outputs the nearest integer.

To obtain an unbiased estimate of the gradient in the estimation step when using the subsampling procedure, we assign weights k/m_g to the subjects sampled from the groups $\mathcal{G}_g$, $g = 1, \ldots, k$, and weight n_0/m_0 to those sampled from $\mathcal{G}_0$, so that each subject has weight 1 divided by the probability of their being sampled. The fact that we can obtain unbiased estimates by using the grouped subsampler is crucial. Many apparently natural subsampling solutions to the column rank problem, e.g. the solution that samples subjects until the matrix has full column rank, will not work because they produce samples that cannot easily be weighted to obtain unbiased estimates.

4.5. Prediction

Suppose that, for a given subject i, we want to predict the value of the latent process at a given time t_k, i.e. $Y_{ik}^* = \mathbf{x}_{ik}^{\mathrm{T}} \boldsymbol{\beta} + \mathbf{d}_{ik}^{\mathrm{T}} \mathbf{U}_i + W_i(t_k)$. Different types of predictions may be defined depending on the scientific interests of a specific application. The first is smoothing prediction, where the quantity of interest is the value given all available data for that patient, $Y_{ik}^{*}|\mathbf{Y}_i$. The second is filtering, where the quantity of interest is the value given all data collected before the time t_k, $Y_{ik}^{*}|\mathbf{Y}_i^{k,f}$, where $\mathbf{Y}_i^{k,f}=\{Y_{ij}:t_{ij}<t_k\}$. The third is nowcasting, where the quantity of interest is the value given all data collected up to and including the time t_k, $Y_{ik}^{*}|\mathbf{Y}_i^{k,n}$, where $\mathbf{Y}_i^{k,n}=\{Y_{ij}:t_{ij}\leqslant t_k\}$.

For all three cases, we can sample from the relevant predictive distribution, $Y_{ik}^{*}|\mathbf{Y}_i^{\star}$, using the same Gibbs sampler that was used when estimating the gradient (just conditioning on different sets of data). The details of this Gibbs sampler are given in Appendix A.1. Given M values obtained from the Gibbs sampler, we approximate the quantities of interest such as the predictive mean or the quantiles of the predictive distribution needed for constructing prediction intervals, using MC integration.

5. Model validation and model selection

An obvious question is how to decide when a non-Gaussian model is preferable to the standard Gaussian model. A natural first step would be to check the validity of a Gaussian model through its marginal residuals, $Y_{ij}-\mathbf{x}_{ij}^{\mathrm{T}}\boldsymbol{\beta}$, standardized by their variances. These standardized residuals can be plotted against theoretical quantiles of the standard normal distribution to check for departures from normality. However, this plot would not show which of the model components are the source of the non-Gaussianity. Also, deviations from normality in such a plot do not necessarily indicate that a non-Gaussian model is needed. Consider for example data from the very simple longitudinal model $Y_{ij}=U_i+Z_{ij}$, where $U_i\sim N(0,\sigma_U^2)$ and $Z_{ij}\sim N(0,\sigma_z^2)$ are independent. If the time series for each subject are sufficiently long, the quantile–quantile (Q–Q)-plot of Y_{ij} can deviate substantially from normality because the value of U_i is replicated over the entire time series. Finally, the approach cannot easily be used to check the validity of any given non-Gaussian model, since we do not necessarily know the true distribution of its residuals.

We therefore check the validity of a model, Gaussian or not, by predicting each model component from the data given the estimated parameters and compare the distribution of each component with the corresponding quantity for data simulated from the model. Thus, to check the validity of the error model, we compute $\hat{Z}_{ij}=Y_{ij}-\mathbf{x}_{ij}^{\mathrm{T}}\boldsymbol{\beta}-E[U_i+W_i(t_{ij})|\mathbf{Y}_i]$, then simulate Y_{ij}^{s} according to the model and compute $\hat{Z}_{ij}^{s}=E[Z_{ij}|\mathbf{Y}^{s}]$ based on the simulated values. We can then visualize the model fit by using, for example, Q–Q-plots between $\hat{Z}_{ij}$ and $\hat{Z}_{ij}^{s}$. If these plots deviate from the line of equality, this indicates that the model does not fit the data. For a more formal assessment, we can repeat the procedure for K different simulated data sets and compute a joint simulation envelope. If the envelope does not contain the line of equality we can reject that the data are generated by the model.

Using the same simulations, we can similarly assess the fit of the random effects U_i, comparing the quantiles of $\hat{U}_i=E[U_i|\mathbf{Y}_i]$ and $\hat{U}_i^{s}=E[U_i|\mathbf{Y}^{s}]$. To assess the fit of the process $W_i(t)$, we apply a similar procedure to the innovations of the process $\mathrm{d}L_i$. Using the innovations, rather than the $W_i(t)$, avoids the correlation-induced distortion of the empirical marginal distributions of $W_i(t)$.

6. Case-studies

6.1. Natural progression of lung function in cystic fibrosis patients

Our first application uses data on the lung function of cystic fibrosis patients, taken from the Danish cystic fibrosis register. The patients are all aged over 5 years and entered the database between 1969 and 2010. The outcome variable is %FEV1 (percentage predicted forced expiratory volume in 1 s), which is a measure of lung function that is widely used as a descriptor of

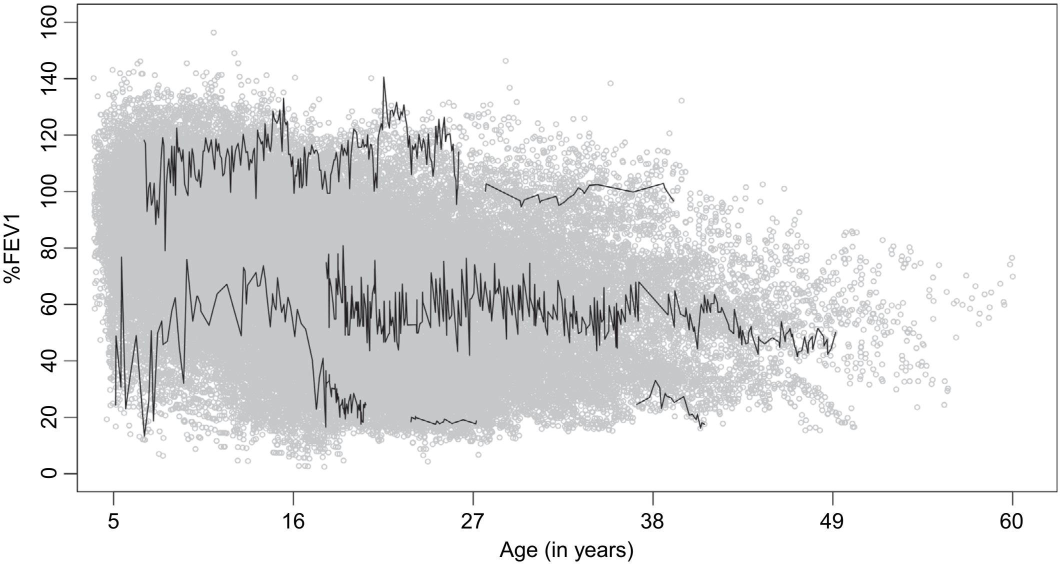

Fig. 4. %FEV1 measurements against age (in years) in the background as a grey scatter plot: ———, data on six patients

severity of disease (Davies and Alton, 2009). The data, previously analysed by Taylor-Robinson *et al.* (2012), contain 70448 measurements of %FEV1 on 479 patients with follow-up times approximately 1 month apart. For the analysis that is reported here, three patients who provided only one %FEV1-measurement have been excluded. Hence, 476 patients are available for the current analysis. Available covariates are sex, age, birth cohort (decadal), presence or absence of pancreatic sufficiency, presence or absence of *diabetes mellitus* and the number of years with pseudomonas: a bacterial infection to which cystic fibrosis patients are susceptible. The number of repeated measures per patient ranges between 2 and 597 with a median of 101.5. Total follow-up times range between 0.1 and 31.5 years with a median of 10.5. Of the 476 patients, 233 (48.9%) are female, 20 (4.2%) have pancreatic sufficiency and 14 (2.9%) have diabetes. Baseline ages range between 5.0 and 48.1 years with a median of 7.0 years. Cohort numbers are 7 (1.5%), 42 (8.8%), 109 (22.9%), 105 (22.1%), 141 (29.6%) and 72 (15.1%) for birth cohorts of 1948–1957, 1958–1967, ..., 1998–2007 respectively. Baseline %FEV1 values range between 10.4 and 140.3 with a mean of 78.5. Fig. 4 shows traces for six patients, chosen to illustrate a range of total follow-up times and patterns of the outcome variable %FEV1.

Fitting a model to these data serves two purposes. The first is to characterize the mean response profile of lung function in cystic fibrosis patients, adjusted for relevant covariates. The second is to quantify the extent to which a subject's early results are predictive of their long-term prognosis.

We consider %FEV1 as the outcome Y and specify mixed effects models that fall within the general framework of equation (9). Specifically, we consider

$$Y_{ij} = \mathbf{x}_{ij}^{\mathrm{T}}\boldsymbol{\beta} + U_i + W_i(t_{ij}) + Z_{ij}, \tag{21}$$

where each $\mathbf{x}_{ij}$ contains a number of explanatory variables, as listed in Table 3. We model $W_i(t)$ as the solution to the stochastic differential equation $(\kappa^2 - d^2/dt^2)W_i(t) = \mathrm{d}L_i(t)$, which implies that $W_i(t)$ has a Matérn covariance function with smoothness parameter $\frac{3}{2}$. We also considered

Table 3. Estimates of the fixed effects for the normal and NIG models†

	Results for the normal model			*Results for the NIG model*		
	Estimate	*Standard error*	*p-value*	*Estimate*	*Standard error*	*p-value*
Intercept	68.23	2.07	< 0.001	72.98	2.06	< 0.001
Diabetes	−3.05	0.52	< 0.001	−1.76	0.44	< 0.001
Years after pseudomonas infection	−0.46	0.08	< 0.001	−0.45	0.07	< 0.001
Age	−0.25	0.08	0.002	−0.47	0.07	< 0.001
cohort 1948	1.71	10.09	0.865	2.83	9.54	0.767
cohort 1958	−4.05	3.97	0.308	−8.12	3.82	0.034
cohort 1978	18.21	2.93	< 0.001	14.5	2.87	< 0.001
cohort 1988	26.37	2.84	< 0.001	22.52	2.74	< 0.001
cohort 1998	28.95	3.59	< 0.001	23.28	3.34	< 0.001
Pancreatic sufficiency	0.98	6.26	0.876	4.26	5.71	0.456
Age ∗ cohort 1948	−0.08	0.19	0.674	−0.06	0.17	0.724
Age ∗ cohort 1958	0.09	0.08	0.261	0.28	0.07	< 0.001
Age ∗ cohort 1978	−0.83	0.09	< 0.001	−0.71	0.09	< 0.001
Age ∗ cohort 1988	−0.79	0.15	< 0.001	−0.81	0.14	< 0.001
Age ∗ cohort 1998	0.49	0.54	0.364	0.35	0.43	0.416
Age ∗ pancreatic sufficiency	1.12	0.3	< 0.001	0.81	0.27	0.003

†Age is centred at 5. Cohort 1968, absence of diabetes and absence of pancreatic sufficiency are the reference categories.

a model with an exponential covariance function, as in Taylor-Robinson *et al.* (2012), but this gave a worse fit to the data.

In this example, cohort effects are substantial, reflecting general improvements in the treatments that are available to cystic fibrosis patients over the time period that is concerned. This, coupled with the small numbers of patients in some cohorts (e.g. seven patients in 1948–1957), explains why the grouped subsampler that was described in Section 4.4 is needed.

To illustrate the effect of the subsampling using the proposed grouped subsampler, we first fit a Gaussian model, i.e. assuming Gaussian distributions for U_i, $W_i(t)$ and Z_{ij}, with and without subsampling. In the former case, we subsample 20% of the patients, i.e. 96 out of 476. The resulting parameter tracks of the optimizer (for six of the model parameters) can be seen in Fig. 3. In this example, there are $k = 7$ subsampling groups, with an average group size of eight subjects, and we sampled two groups at each iteration. The running time for each iteration scales linearly with M, the number of patients who are subsampled at each iteration. Thus, subsampling reduces computing time per iteration by a factor of almost 5 in this case. However, since 17000 iterations were needed to meet the convergence criteria with subsampling, compared with 6000 iterations without, the total computation time was reduced by a factor of 1.75. The variances of the subsampled estimates are slightly larger, but the final parameter estimates are almost identical. For applications with data for many more subjects, e.g. as in the renal case-study to be presented in the next section, the computational gain by subsampling would be larger.

To assess the suitability of the Gaussian distributional assumption, we inspected Q–Q-plots of the standardized marginal residuals, $Y_{ij} - \mathbf{x}_{ij}^{\mathrm{T}}\boldsymbol{\beta}$. Fig. 5 suggests some departure from the Gaussian distribution but, as each marginal residual is composed of U_i, $W_i(\cdot)$ and Z_{ij}, the Q–Q-plot cannot detect the source of the departure. We therefore also look at the Q–Q-plots for the various model components, as explained in Section 5. The results for the Gaussian model can be seen in Figs 6(a)–6(c). The normality assumption seems to be valid for the random effects

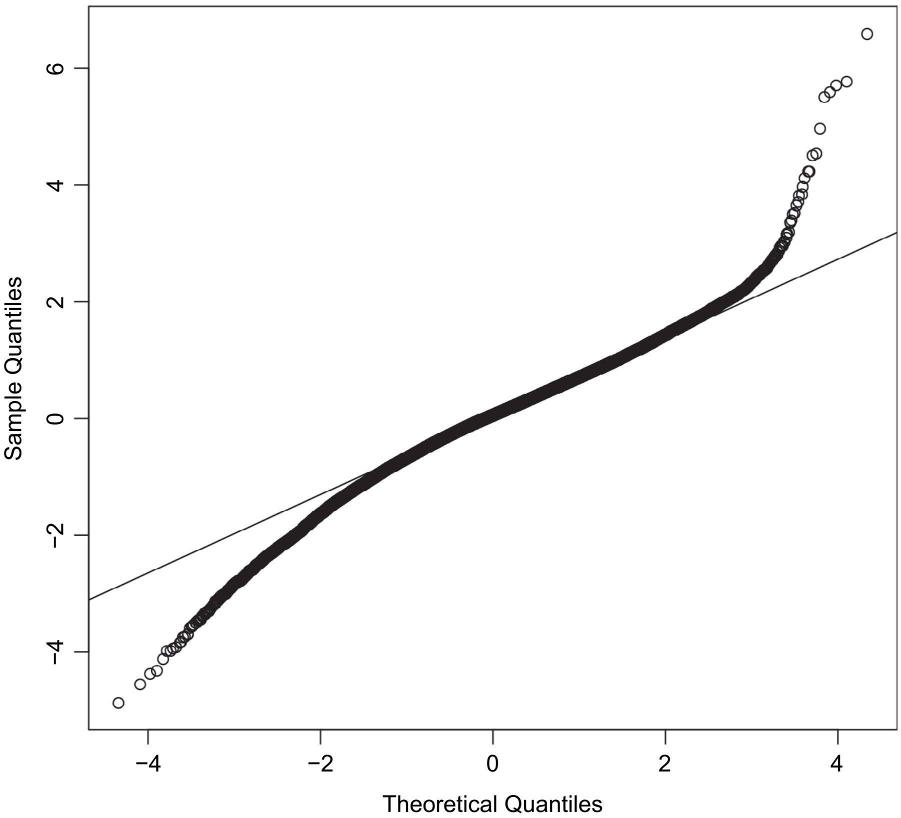

Fig. 5. *Q–Q*-plot of standardized residuals under the Gaussian assumption for the cystic fibrosis example

U_i, but both the process $W_i(\cdot)$ and the errors Z_{ij} seem to have departures from the normal distribution. On the basis of these, we fitted a model with the NIG assumption for $W_i(\cdot)$ and Z_{ij} and normal distribution assumption for U_i. The corresponding Q–Q-plots for this model form Figs 6(a)–6(f). All three components now fit fairly well, although the random effects for the data seem to have a slightly skewed distribution. Thus, as a final model we fitted a model with an NIG assumption for each of the three model components. Figs 6(g)–6(i) show the Q–Q-plots for this model. The NIG assumption for the random effects improves the fit that the distributional assumptions are now reasonably good for all three components. We conclude that the NIG assumption for all three stochastic components is the most appropriate model for these data.

The estimates of the fixed effect parameters $\boldsymbol{\beta}$ for the normal and NIG models are shown in Table 3. Standard error estimates, obtained by using the observed Fisher matrix, are generally lower under the NIG than under the Gaussian assumption. With regard to statistical significance, p-values indicate the same judgement on significance, except for pancreatic sufficiency, main effect of cohort 1958–1967 and its interaction with age. Note that both pancreatic sufficiency and cohort 1958–1967 are highly unbalanced with only 20 positive out of 476 and only 42 subjects in the 1958–1967 cohort.

In Section 7.1, we report the results from a simulation study to validate these findings. Two important conclusions based on the simulation study are that

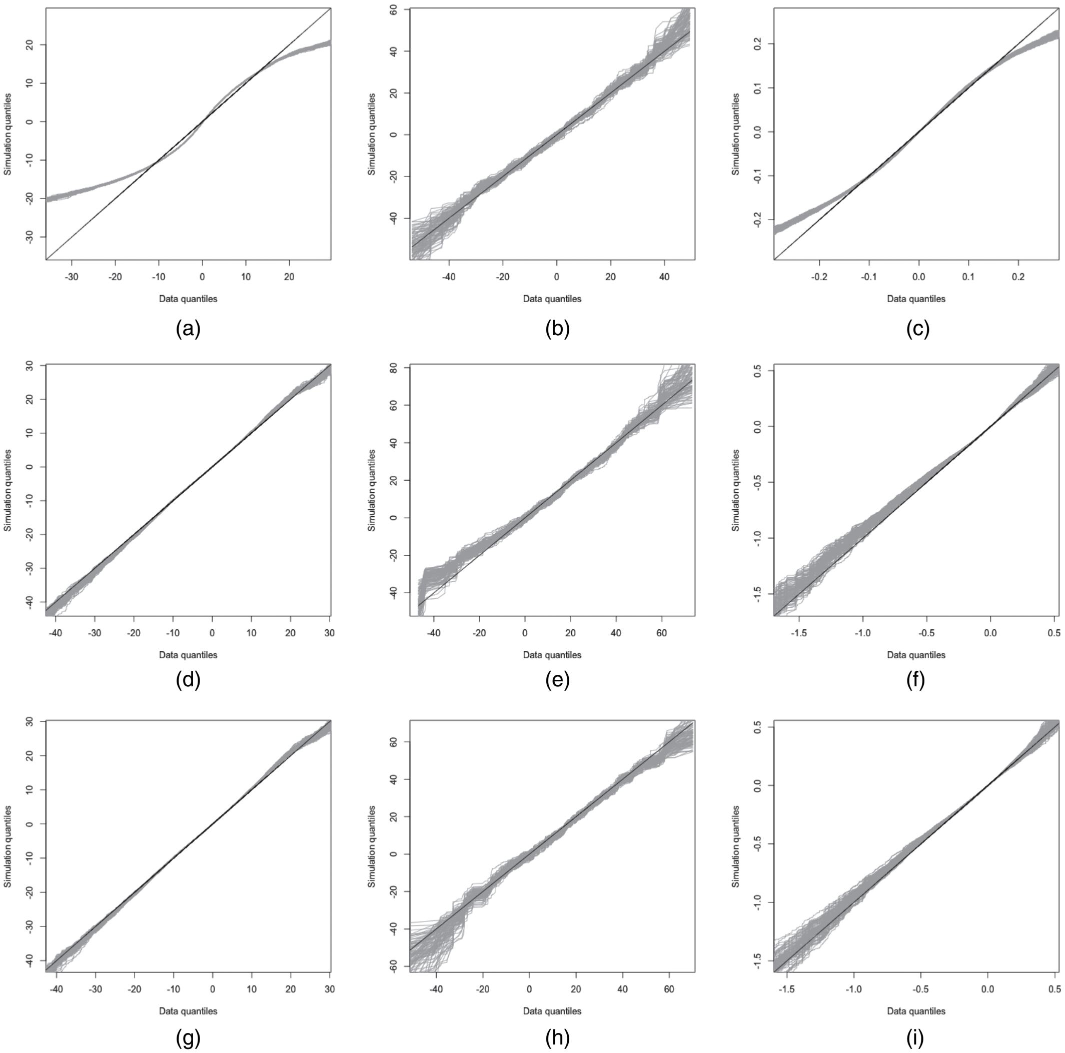

(a) (b) (c)

(d) (e) (f)

(g) (h) (i)

Fig. 6. *Q–Q*-plots for the components of the models in Section 6.1 for the cystic fibrosis example, based on 100 simulated data sets from each model: for the model with Gaussian (a) Z_{ij}, (b) U_i and (c) $W_i(t)$; for the model with (d) NIG-distributed Z_{ij}, (e) Gaussian U_i and (f) NIG-distributed $W_i(t)$; for the model with NIG distributions for (g) Z_{ij}, (h) U_i and (i) $W_i(t)$

(a) it is important to include a random-process term $W_i(t)$ in the model to obtain reliable inferences for the fixed effects and

(b) a Gaussian assumption for $W_i(t)$ may still deliver reliable inferences regarding fixed effects, when the data show signs of non-Gaussianity.

6.2. Progression towards end stage renal failure

Our second application uses clinical data on kidney function of primary care patients from the northern English city of Salford who are in high-risk groups for chronic kidney disease. The outcome variable is eGFR (estimated glomerular filtration rate, in millilitres per minute per

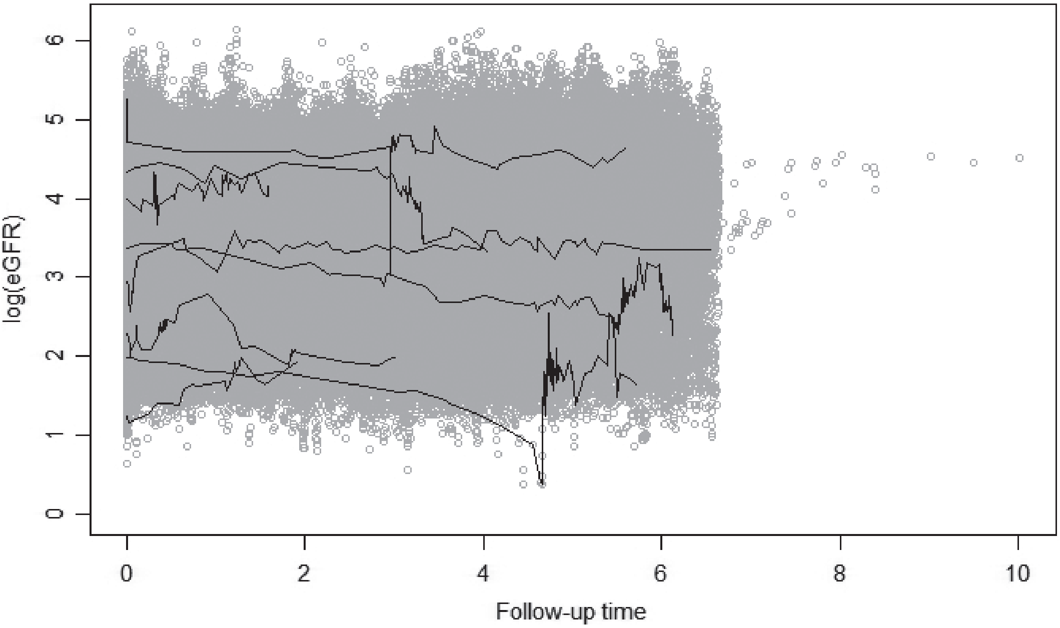

Fig. 7. eGFR-measurements (on a log-scale) against follow-up time (in years) in the background as a scatter plot: data on eight patients are highlighted by black lines connecting successive measurements

1.73 metres squared of body surface area): a proxy measurement for the patient's renal function calculated as

$$\mathrm{eGFR} = 175\left(\frac{\mathrm{SCr}}{88.4}\right)^{-1.154} \mathrm{age}^{-0.203} \,\mathrm{x}\, 0.742^{I(\mathrm{female})/} \mathrm{x}1.21^{I(\mathrm{black})/}, \tag{22}$$

where SCr stands for serum creatinine measured in micromoles per litre (Levey *et al.*, 1999).

The data, which were previously analysed by Diggle *et al.* (2015), contain a total of 392870 measurements on 22910 patients, for whom the total follow-up time ranged from 0 (i.e. only baseline data are available) to 10.0 years, whereas the number of measurements of eGFR ranged from 1 to 305. Among the 22910 patients, 11833 (51.7%) were male. Baseline ages ranged between 13.7 and 102.1 with a mean of 65.4.

Fig. 7 shows traces for eight patients, chosen to illustrate some particularly challenging features of the data. The unusually high degree of irregularity in the follow-up times reflects the fact that the data derive from routine clinical practice. In particular, some patients provided many repeated measurements over a relatively short time period, probably during episodes of intercurrent illness.

Clinical care guidelines in the UK include a recommendation that any person in primary care who appears to be losing kidney function at a relative rate of at least 5% per year should be considered for referral to specialist secondary care. Our primary objective in analysing these data is therefore to develop a method for identifying, for each subject and in realtime, when this criterion is first met.

As in Diggle *et al.* (2015), we use a log-transformed outcome variable $Y = \log(\mathrm{eGFR})$ and specify a model of the form

$$Y_{ij} = \mathbf{x}_{ij}^{\mathrm{T}}\boldsymbol{\beta} + U_i + W_i(t_{ij}) + Z_{ij}. \tag{23}$$

In model (23), each $\mathbf{x}_{ij}$ includes sex, baseline age, follow-up time t_{ij} and a piecewise linear function of age with a slope change at age 56.5 years. The processes $W_i(t)$ are integrated random walks as in Diggle *et al.* (2015).

As for the previous example, we first fit the model under Gaussian assumptions for the U_i-, $W_i(\cdot)$- and Z_{ij}-components. The Q–Q-plot for the standardized residuals that are shown as Fig. 5 of Diggle *et al.* (2015) clearly indicates longer-than-Gaussian tails. As for the cystic fibrosis case-study, we compute the Q–Q-plots for each model component (Fig. 8), which suggest that the Gaussian assumption is not valid for any of the model components. Therefore, we proceed by assuming NIG distributions for each of the three stochastic components. The fit is much improved, albeit with some discrepancy between the data and model in the lower tail of the U_i and the upper tail of the $W_i(t)$.

Fig. 9 shows, for two patients, their observed data and the concurrent ('nowcasting') probabilities of meeting the clinical guideline for referral to specialist care. Results are shown for the Gaussian and NIG models. As would be expected, for each patient the general pattern of the predictive probabilities is similar under both modelling assumptions, but there are some substantial quantitative differences and the ranking of each pair of predictive probabilities is not consistent. The two sets of model-based predictions reflect different partitionings of the intrapatient variation into signal and noise components, and the balance between the two is affected in subtle ways by the pattern of follow-up times and their associated measurements.

To put these differences in context, in Section 7.2 we report the results of a simulation study, where we find that the distributional assumptions have a strong effect on the predictive performance.

7. Simulation studies

7.1. Fixed effects estimation

We conduct a simulation study to investigate the extent to which distributional assumptions affect the validity and/or efficiency of estimators for $\boldsymbol{\beta}$. We focused on evaluating the bias and coverage properties of the estimators by using the models for the cystic fibrosis patients that were presented in Section 6.1, but with a reduction in size to 256 patients covering the cohorts between 1958 and 1978 to reduce computation time.

We consider two simulation models, denoted normal and NIG. In the first, all three stochastic components are Gaussian, with parameters set at the estimates that were obtained from the cystic fibrosis data, whereas in the second all three stochastic components are NIG distributed, again with parameters set at their estimates from the cystic fibrosis data; see Table 3 for $\boldsymbol{\beta}$ and Table 4 for the parameters of U_i, $W_i(t)$ and Z_{ij}. We generate 250 replicate data sets from each of the two simulation models. For each data set we fit both simulation models and three additional 'wrong' Gaussian models: a standard multiple linear regression model, a random-intercept-only model and a random-intercept and random-slope model. In each case, we evaluate the empirical bias of each parameter estimator and the coverage of nominal 90% confidence intervals over the 250 replicates. The confidence intervals are computed as explained in Section 4.3. The results are presented in Tables 5 and 6. Important findings are as follows.

(a) For both the normal and the NIG simulation models, the linear regression model and the two random-effects models give very poor coverages, indicating that inclusion of the process component $W_i(t)$ is crucial for making correct inferences about the fixed effects.

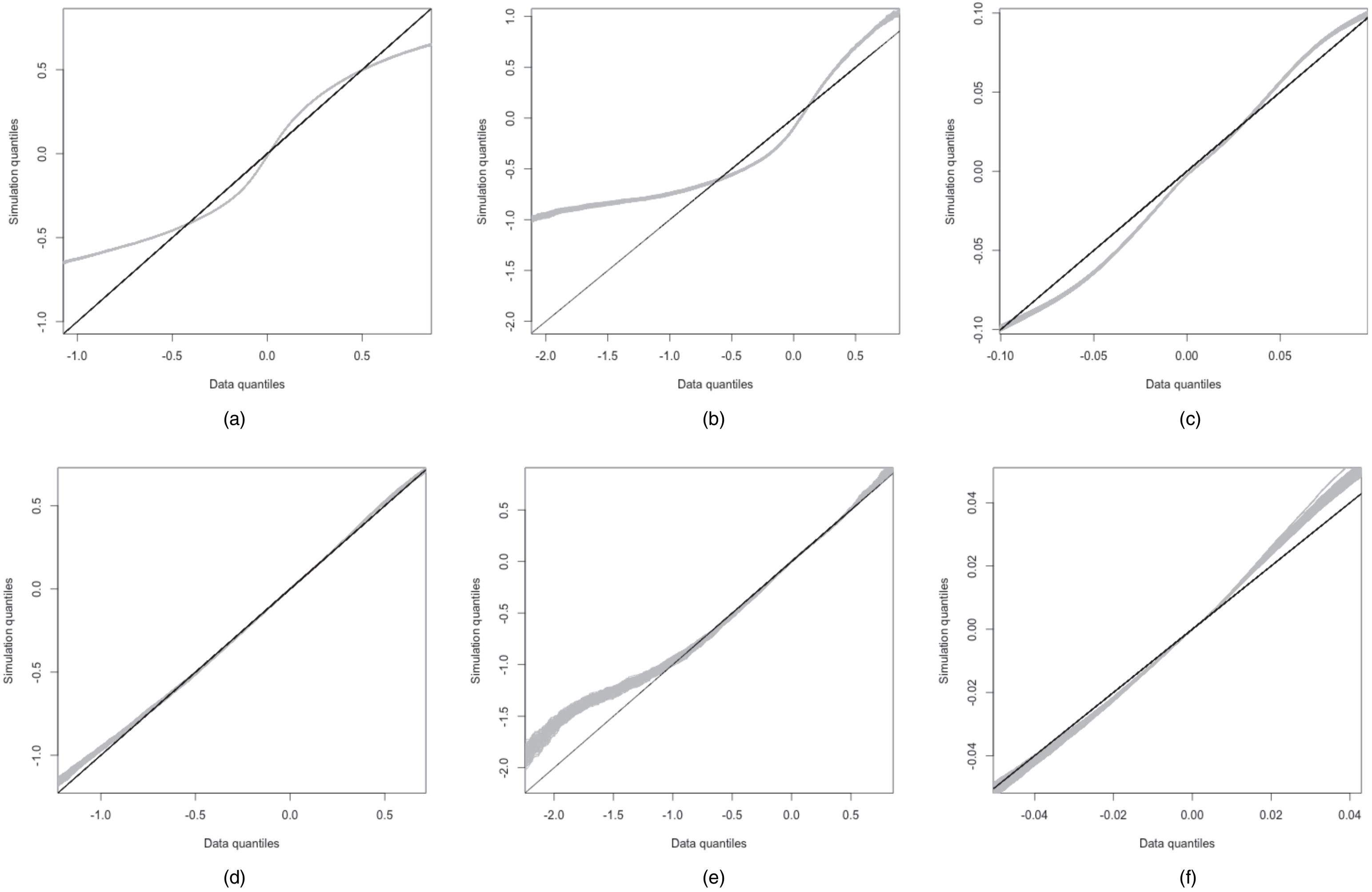

(a) (b) (c)

(d) (e) (f)

Fig. 8. *Q*–*Q*-plots for the three model components of the (a)–(c) Gaussian and (d)–(f) NIG models for the renal failure data: (a) normal Z_{ij}; (b) normal U_i; (c) normal $W_i(t)$; (d) NIG Z_{ij}; (e) NIG U_i; (f) NIG $W_i(t)$

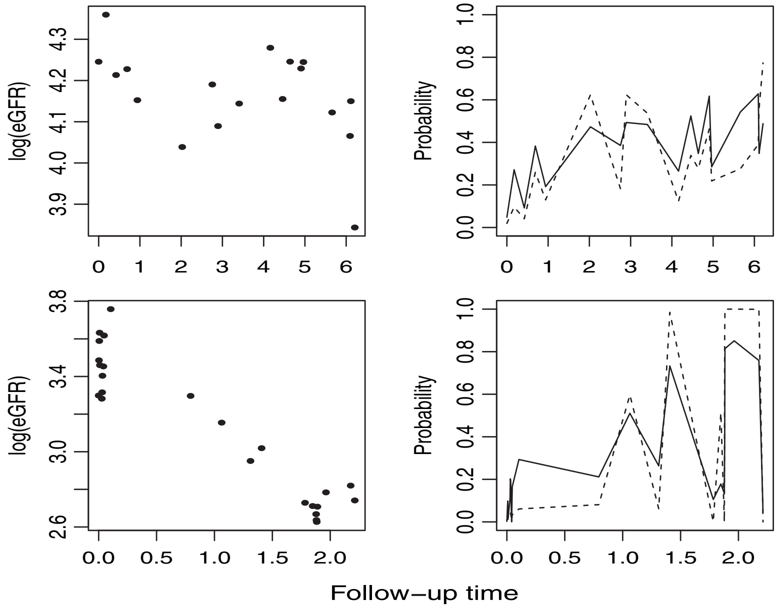

(a) (b)

Fig. 9. (a) follow-up time (in years) *versus* log(eGFR) for two patients and (b) probabilities of meeting the clinical guideline for the patients (———, normal distribution; – – –, NIG distribution)

Table 4. Parameters for U_i, $W_i(t)$ and Z_{ij} used in the simulation study

Model	Σ^U	μ^U	ν^U	σ^Z	μ^Z	ν^Z	τ	κ	μ^W	ν^W
Normal	341.59			6.76			0.10	1.22		
NIG	294.36	−47.24	19.26	6.59	−1.16	0.52	0.089	1.21	−0.08	0.34

(b) For the normal simulation model, the performances of the NIG model and the normal model are similar, indicating that the NIG model gives reliable estimates even if the data are Gaussian.

(c) For the NIG simulation model, the confidence intervals for the normal model have almost the correct coverage. The NIG model has similar coverage and bias to those for the normal model. However, the standard deviations of the estimates for the NIG model are smaller in the case of NIG data, which makes the confidence intervals tighter and thus indicates that we obtain a higher efficiency when using the NIG model when the data are non-Gaussian.

The overall conclusion from this small simulation study is that it is important to include a random process in the model to obtain reliable inference of the fixed effects but that, for this purpose, a Gaussian model can give reliable inferences even if the data show signs of being non-Gaussian.

7.2. Prediction accuracy

To study the importance of the distributional assumptions on prediction, we perform a simulation study based on the renal failure application, presented in Section 6.2. We simulate new data

Table 5. Results for the simulation study on fixed effects estimation†

	Results for the linear model			*Results for the random model*			*Results for the random-slope model*			*Results for the normal model*			*Results for the NIG model*		
	Bi	*C*	*Se*	*Bi*	*C*	*Se*	*Bi*	*C*	*Se*	*Bi*	*C*	*Se*	*Bi*	*C*	*Se*
Intercept	−1	15	0.28	−1	84	1.89	−1	82	1.99	−1	90	2.04	−1	85	1.99
Diabetes	−4	8	0.27	−1	30	0.22	−1	24	0.27	2	90	0.58	2	88	0.58
Years after pseudomonas infection	2	11	0.02	1	25	0.02	1	77	0.08	0	90	0.08	−1	88	0.08
Age	−3	14	0.02	−2	25	0.02	−1	27	0.03	0	92	0.08	1	92	0.08
cohort 1958	−7	16	0.62	6	82	3.56	9	73	3.7	4	88	3.91	3	86	3.79
cohort 1978	2	16	0.47	2	85	2.67	2	79	2.77	2	89	2.89	2	85	2.79
Pancreatic sufficiency	−17	17	2.91	−13	65	6.92	−10	67	7.16	−3	93	10.43	−3	93	10.42
Age * cohort 1958	−14	16	0.03	8	20	0.02	13	33	0.05	5	89	0.08	5	88	0.08
Age * cohort 1978	1	19	0.03	0	30	0.02	0	29	0.04	0	95	0.09	0	96	0.09
Age * pancreatic sufficiency	2	20	0.16	3	36	0.16	3	34	0.16	2	94	0.42	2	92	0.43

†250 data sets are generated from the normal model. Bi, percentage relative bias (the bias divided by the true parameter times 100); *C*, percentages of the 90% confidence intervals that cover the true value; Se, standard deviations of the estimates.

Table 6. Results for the simulation study on fixed effects estimation†

	Results for the linear model			*Results for the random model*			*Results for the random-slope model*			*Results for the normal model*			*Results for the NIG model*		
	Bi	*C*	*Se*	*Bi*	*C*	*Se*	*Bi*	*C*	*Se*	*Bi*	*C*	*Se*	*Bi*	*C*	*Se*
Intercept	0	10	0.31	0	85	2.08	0	83	2.22	0	92	2.26	0	90	2.16
Diabetes	−1	8	0.3	−3	24	0.24	−9	27	0.3	−1	89	0.62	0	90	0.47
Years after pseudomonas infection	2	7	0.02	−3	27	0.02	−2	73	0.09	−1	92	0.09	0	89	0.07
Age	−2	13	0.02	3	25	0.02	2	32	0.03	1	90	0.09	1	86	0.07
cohort 1958	0	13	0.68	−2	84	3.91	−2	71	4.1	−2	88	4.34	−2	87	3.99
cohort 1978	2	13	0.52	1	83	2.94	2	82	3.07	2	88	3.2	2	88	2.96
Pancreatic sufficiency	−18	21	3.21	16	61	7.62	15	62	7.98	11	89	11.75	9	86	10.25
Age * cohort 1958	1	14	0.03	1	22	0.02	−2	27	0.06	−1	94	0.09	−1	90	0.07
Age * cohort 1978	1	27	0.04	0	27	0.02	1	24	0.04	0	87	0.1	1	86	0.08
Age * PS	3	17	0.18	−3	35	0.18	−3	32	0.17	−2	88	0.49	−1	90	0.4

†250 data sets are generated from the NIG model. For the explanations, see the caption of Table 5.

from the fitted NIG model, for the two patients who are shown in Fig. 9. For each simulated sequence $Y_{ij} = \log(\text{eGFR})$ at follow-up times t_{ij}, we then use the fitted NIG and Gaussian models that were reported in Section 6.2 to obtain the nowcasting predictions. Table 7 shows the results based on 100 simulated data sets, using four summaries of predictive performance: the mean absolute error MAE; root-mean-squared error RMSE; mean coverage of 95% prediction intervals, COV, and the average width of these prediction intervals, Width. For the two models, we also look at the model-based predictive probabilities of meeting the clinical guideline for referral to specialist care, and we compare these with the corresponding known values of log-transformed

Table 7. Results for the simulation study for prediction†

Model	*MAE* (× *100*)	*RMSE* (× *100*)	*COV*	*Width*	*AUC*
Normal	9.122	2.705	0.912	0.402	0.959
NIG	5.849	0.838	0.935	0.283	0.995

†The results are based on 100 simulated data sets for the two patients for whom results are presented in Fig. 9.

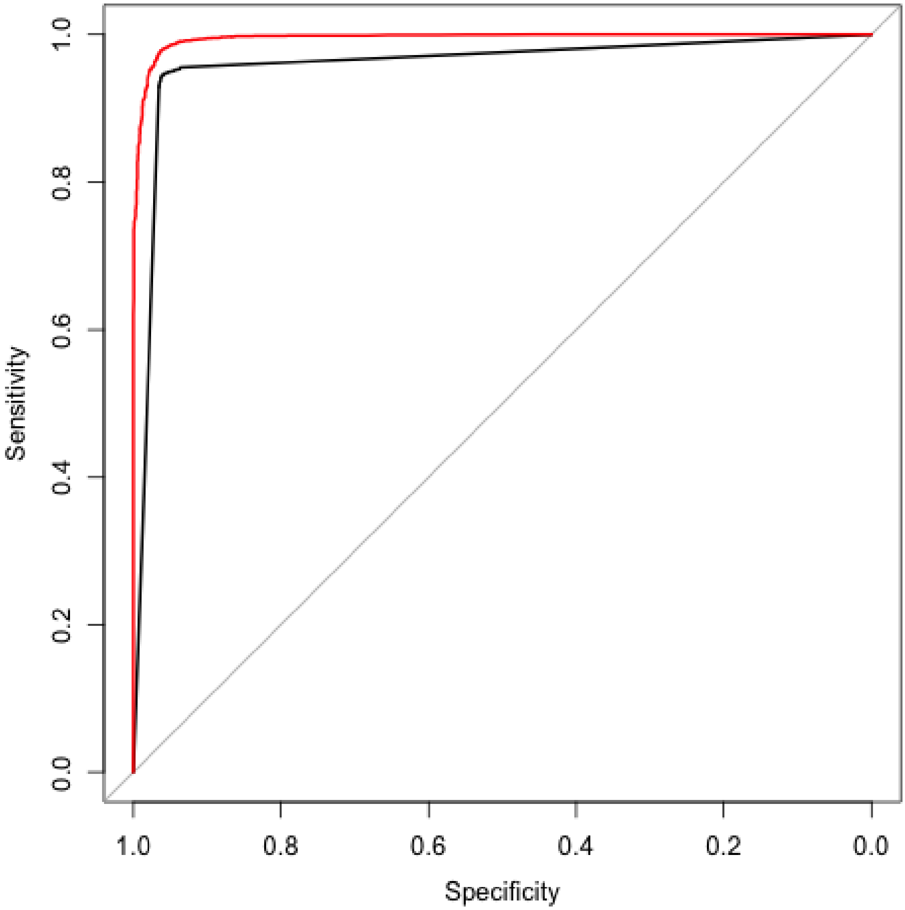

Fig. 10. Receiver operating characteristic curves: ———, Gaussian model; ———, NIG model

GFR. This comparison is summarized by using the receiver operating characteristic curves in Fig. 10 and the area under the curve, AUC, which ideally should be 1. There is a substantial increase in predictive power, according to all measures of accuracy, when the correct model, the NIG model, is used.

8. Software

We have implemented the methodology that is presented in this paper in the R package `ngme`. A development version of the package is available from `https://bitbucket.org/davidbolin/ngme`. The package includes functions for parameter estimation and for subject level prediction using the class of models defined by expression (9), with the following features.

(a) Any linear model can be specified for the regression term $\mathbf{x}_{ij}^{\mathrm{T}}\boldsymbol{\beta}$ and for the subject level random effect $\mathbf{d}_{ij}^{\mathrm{T}}\mathbf{U}_i$, using the standard R model formula syntax.
(b) The random-effects distribution can be chosen as normal or NIG.
(c) The covariance structure of the $W_i(t)$ can be specified as a stationary, exponentially correlated process (the fully asymmetric version), as a symmetric or asymmetric Matérn model with smoothness 1.5, or as a non-stationary integrated random walk or omitted altogether to give non-Gaussian versions of the Laird–Ware model. The distribution for the process can be specified as normal, NIG, GAL or Cauchy.
(d) The distribution of the measurement error terms can be specified as normal, NIG or t.
(e) Subject level predictions can be obtained either through nowcasting (conditioning on a subject's past and current measurement data), smoothing (conditioning on all of a subject's data) or forecasting (conditioning on all of a subject's past data).

The generic R functions, `print`, `summary`, `plot`, `fitted` and `residuals` are available for the estimation and prediction functions, and the renal data set is included. We plan to extend the package's functionality to a wider range of models for the stochastic process component $W_i(t)$, including a general Matérn correlation structure. The package also has support for estimation of non-Gaussian models for spatial data as we discuss further in the next section.

9. Discussion

The Gaussian version of the linear mixed model (9) represents the standard approach to analysing real-valued repeated measurement data. Typically, the simplified version without the Gaussian process term $W_i(t)$ suffices when the number of follow-up times per subjects is small, whereas the version with the $W_i(t)$ term, often in conjunction with a simple random intercept U_i in place of the general term $\mathbf{d}_{ij}^{\mathrm{T}}\mathbf{U}_i$, usually gives a better fit to data with long follow-up sequences. Concerns have often been raised about the legitimacy of the Gaussian assumption, and in particular about the consequences of fitting Gaussian models when elements of the underlying process have longer-than-Gaussian tails or skewness. This has led to an extensive literature, which we reviewed in Section 2. However, to the best of our knowledge the current paper is the first to provide a flexible implementation in which departure from Gaussianity can be assessed independently for each of the three stochastic components of model (9).

In our reanalysis of the cystic fibrosis data, inferences on fixed effects showed only small changes when non-Gaussian behaviour is taken into account. Our reanalysis of the renal data also finds evidence of non-Gaussian behaviour, which in this case matters more, because it has a material effect on predictive inference, and hence on the point at which an individual patient in primary care would be considered for referral to secondary care.

We have emphasized the importance of building a computationally efficient algorithm for routine maximization of the likelihood. This is especially useful for data sets containing many subjects. Arguably, computational efficiency is of secondary importance in confirmatory analysis. Once the statistical analysis protocol has been determined, it matters little whether it takes minutes, hours or days of computing time to analyse a data set that typically will have taken weeks, months or years to collect. However, during the iterative model building cycle that characterizes exploratory data analysis, an inability to fit and compare different models in realtime is a severe impediment.

The applications that were described in Section 6 show that the subsampling scheme that was introduced in Section 4.4 can perform very well. One topic of future research is a more thorough investigation of how to optimize the subsampling.

Generalized linear mixed models provide a framework for handling non-Gaussian sampling distributions. This form of non-Gaussian behaviour is complementary to the kind of non-Gaussian process behaviour that we have addressed in this paper. A natural extension to our proposed models would be to generalized linear mixed models for binary or count data with non-Gaussian random effects. However, non-Gaussian behaviour will naturally be more difficult to detect from count or binary data than from measurement data. Binary data in particular can be considered as a heavily censored version of measurement data. For example, a logistic regression model can be interpreted as a linear regression model for a real-valued response Y in which only the sign of Y is observed.

Clinical repeated measurement data are often coupled with time-to-event outcomes, e.g. death. So-called *joint models* for repeated measurement and time-to-event outcomes have been widely studied; for a recent book length account, see Rizopoulos (2012). However, essentially all of this literature assumes that any random-effect components are Gaussian. A natural way of extending the methodology that is presented in this paper to joint modelling problems, by analogy with much of the current literature on Gaussian joint models, would be to combine the linear mixed model (9) with a log-linear Cox process model for the time-to-event outcome, in which the stochastic process $W_i(t)$ in the repeated measurement submodel is correlated with a second stochastic process, $W_i^*(t)$ say, such that $\exp\{W_i^*(t)\}$ constitutes a time-dependent frailty for the ith subject.

Another possible extension of the methodology that is presented in this paper would be to multivariate settings, in which more than one repeated biomarker measurement is collected for each patient, sometimes with different follow-up schedules for different biomarkers. Such models could be constructed similarly to the multivariate random fields in Bolin and Wallin (2020). The models of Bolin and Wallin (2020) are not considered in a longitudinal setting but can naturally be extended to this case. This could then be viewed as an extension of the models that are considered in this work, where the temporal stochastic process is replaced by a random field. The `ngme` package has support for such spatial and multivariate models, both for the longitudinal setting and for the classical geostatistical setting.

Acknowledgements

This work has been partially supported by the Swedish Research Council under grant 201604187. The authors are grateful for the valuable comments from reviewers and editors, which resulted in a much improved manuscript. We also thank Kristin Kirchner for helpful discussions regarding the Petrov–Galerkin method.

Appendix A: Details on the parameter estimation and sampling

A.1. Gibbs sampling

In this section we derive the two conditional distributions that are required for the Gibbs sampler. The first of these is the distribution of $\mathbf{X}_i = (\mathbf{U}_i, \mathbf{W}_i)$ given $\mathbf{Y}_i$ and $\mathbf{V}_i = (\mathbf{V}_i^Z, V_i^U, \mathbf{V}_i^W)$, and the second is the distribution of $\mathbf{V}_i$ given $\mathbf{X}_i$ and $\mathbf{Y}_i$. Using the specification of the hierarchical model from Section 4.1 we have that $\mathbf{X}_i|\mathbf{V}_i \sim N(\mathbf{b}_i, \mathbf{Q}_i^{-1})$, where

$$\mathbf{b}_i = \begin{pmatrix} -\boldsymbol{\mu}^U + \boldsymbol{\mu}^U V_i \\ \mathbf{K}^{-1}(-1 + \mathbf{V}_i^W)\mu^W \end{pmatrix},$$

$$\mathbf{Q}_i = \begin{pmatrix} \frac{1}{V_i^U}\boldsymbol{\Sigma}^{-1} & \mathbf{0} \\ \mathbf{0} & \mathbf{K}^{\mathrm{T}} \operatorname{diag}\left(\frac{1}{\mathbf{V}_i^W}\right)\mathbf{K} \end{pmatrix}.$$

We introduce $\tilde{\mathbf{Y}}_i = \mathbf{Y}_i - \mathbf{x}_i^{\mathrm{T}}\boldsymbol{\beta} + \mu^Z - \mu^Z \mathbf{V}_i^Z$ and $\mathbf{G}_i = (\mathbf{d}_i^{\mathrm{T}}, \mathbf{A}_i^{\mathrm{T}})^{\mathrm{T}}$. We then have $\tilde{\mathbf{Y}}_i|\mathbf{X}_i, \mathbf{V}_i \sim N\{\mathbf{G}_i\mathbf{X}_i, \sigma^2 \operatorname{diag}(\mathbf{V}_i^Z)\}$ and straightforward calculations using properties of the multivariate normal distributions give that $\mathbf{X}_i|\mathbf{Y}_i, \mathbf{V}_i \sim N(\tilde{\mathbf{b}}_i, \tilde{\mathbf{Q}}_i^{-1})$, where

$$\tilde{\mathbf{b}}_i = \tilde{\mathbf{Q}}_i^{-1}\left(\mathbf{Q}_i^{-1}\mathbf{b}_i + \sigma^{-2}\mathbf{G}_i^{\mathrm{T}} \operatorname{diag}\left(\frac{1}{\mathbf{V}_i^Z}\right)\tilde{\mathbf{Y}}_i\right), \qquad \tilde{\mathbf{Q}}_i = \mathbf{Q}_i + \sigma^{-2}\mathbf{G}_i^{\mathrm{T}} \operatorname{diag}\left(\frac{1}{\mathbf{V}_i^Z}\right)\mathbf{G}_i.$$

To compute the distribution of $\mathbf{V}_i$ given $\mathbf{X}_i$ and $\mathbf{Y}_i$, we use the following proposition regarding the convolution between a GIG variable and a Gaussian variable.

Proposition 1. Let $V \sim \mathrm{GIG}(p, a, b)$ and $\mathbf{Y}|V \sim N(\boldsymbol{\beta} + \boldsymbol{\mu}v, v\boldsymbol{\Sigma})$ where $\mathbf{Y} \in \mathbb{R}^n$. Then

$$V|\mathbf{Y} \sim \mathrm{GIG}\{v; p - 0.5n, a + \boldsymbol{\mu}^{\mathrm{T}}\boldsymbol{\Sigma}^{-1}\boldsymbol{\mu}, b + (\mathbf{Y} - \boldsymbol{\beta})^{\mathrm{T}}\boldsymbol{\Sigma}^{-1}(\mathbf{Y} - \boldsymbol{\beta})\}.$$

The proof is straightforward and hence has been omitted. Now, note that the density of $\mathbf{V}_i|\mathbf{X}_i, \mathbf{Y}_i$ factorizes as $f(\mathbf{V}_i|\mathbf{X}_i, \mathbf{Y}_i) = f(\mathbf{V}_i^Z|\mathbf{X}_i, \mathbf{Y}_i) f(V_i^U|\mathbf{U}_i) f(\mathbf{V}_i^W|\mathbf{W}_i)$. If $V_i^U \sim \mathrm{GIG}(p^U, a^U, b^U)$, $V_{ij}^Z \sim \mathrm{GIG}(p^Z, a^Z, b^Z)$, and $V_{ij}^W \sim \mathrm{GIG}(p^W, a^W, b^W)$, then the proposition gives that the three independent distributions are

$$V_i^U|\mathbf{U}_i \sim \mathrm{GIG}\left\{p^U - \frac{d^U}{2}, a^U + (\boldsymbol{\mu}^U)^{\mathrm{T}}\boldsymbol{\Sigma}^{-1}\boldsymbol{\mu}^U, b^U + (\mathbf{U}_i + \boldsymbol{\mu}^U)^{\mathrm{T}}\boldsymbol{\Sigma}^{-1}(\mathbf{U}_i + \boldsymbol{\mu}^U)\right\},$$

$$\mathbf{V}_{ij}^Z|\mathbf{X}_i, \mathbf{Y}_i \sim \mathrm{GIG}\left\{p^Z - 0.5, a^Z + \left(\frac{\mu^Z}{\sigma}\right)^2, b^Z + \frac{(Y_{ij} - \mathbf{x}_{ij}\boldsymbol{\beta} + \mathbf{d}_{ij}\mathbf{U}_i - \mathbf{A}_{ij}\mathbf{W}_i)^2}{\sigma^2}\right),$$

$$\mathbf{V}_{ij}^W|\mathbf{W}_i \sim \mathrm{GIG}\{p^w - 0.5, a^W + (\mu^W)^2, b^w + (\mathbf{K}\mathbf{W}_i + \mathbf{h}\mu^W)_j^2\}.$$

A.2. The gradient of the likelihood

In this section we derive the gradient that is needed for estimating the parameters in the model from Section 4.1. We shall use the notation from Appendix A.1 and also assume that $E[V_i^U] = 1$, $E[\mathbf{V}_i^Z] = \mathbf{1}$ and $E[\mathbf{V}_i^Z] = \mathbf{h}_i$, which was previously assumed for parameter identifiability. Recall that the goal is to evaluate the gradient in equation (18), which can be written as a sum over $\nabla_{\boldsymbol{\Theta}} L_i(\boldsymbol{\Theta}; \mathbf{Y}_i)$, which we approximate by using MC integration as

$$\nabla_{\boldsymbol{\Theta}} L_i(\boldsymbol{\Theta}; \mathbf{Y}_i) \approx \frac{1}{N_{\mathrm{MC}}} \sum_{j=1}^{N_{\mathrm{MC}}} \nabla_{\boldsymbol{\Theta}} L_i(\boldsymbol{\Theta}; \mathbf{Y}_i, \mathbf{V}_i^{(j)})$$

where $\mathbf{V}_i^{(j)}$ are samples from $\mathbf{V}_i|\mathbf{Y}_i$ obtained by using the Gibbs sampler above. Thus, what we must derive here is $\nabla_{\boldsymbol{\Theta}} L_i(\boldsymbol{\Theta}; \mathbf{Y}_i, \mathbf{V}_i^{(j)})$. To do this, we shall use that $\nabla_{\boldsymbol{\Theta}} L_i(\boldsymbol{\Theta}; \mathbf{Y}_i, \mathbf{V}_i^{(j)}) = E_{\mathbf{X}_i}[\nabla_{\boldsymbol{\Theta}} L_i(\boldsymbol{\Theta}; \mathbf{Y}_i, \mathbf{X}_i, \mathbf{V}_i^{(j)})|\mathbf{Y}_i, \mathbf{V}_i]$.

To simplify the notation, we let $L_i(\tilde{\boldsymbol{\Theta}}; \mathbf{X}_i, \mathbf{V}_i, \mathbf{Y}_i)$ denote the complete log-likelihood for the ith patient seen as a function of the parameters $\tilde{\boldsymbol{\Theta}}$, and similarly let $L_i(\tilde{\boldsymbol{\Theta}}|\mathbf{V}_i, \mathbf{Y}_i)$ denote the log-likelihood conditioned on the variance components. To derive the gradients, we also need the following notation from matrix calculus. The *vec* operator transforms a matrix into a vector by stacking its columns. The *vech* operator also transforms an $n \times n$ matrix into a vector but removes all the subdiagonal elements. Finally, the duplication matrix $\mathbf{D}_n$ is such that, for any symmetric matrix $\mathbf{A}$, $\mathbf{D}_n \operatorname{vech}(\mathbf{A}) = \operatorname{vec}(\mathbf{A})$.

We start by deriving the gradients for the fixed effect and the asymmetric parameters. Let $(\boldsymbol{\beta}, \boldsymbol{\mu}) = (\boldsymbol{\beta}, \boldsymbol{\mu}^U, \mu^Z, \mu^W)$ and $\mathbf{B}_i = (\mathbf{x}_i, \mathbf{d}_i(-1 + V_i^U), (-1 + \mathbf{V}_i^Z), \mathbf{A}_i\mathbf{K}^{-1}(-\mathbf{h}_i + \mathbf{V}_i^W))$. Using the model definition from Section 4.1, we have that

$$L_i\{(\boldsymbol{\beta}, \boldsymbol{\mu}), \sigma; \mathbf{X}_i, \mathbf{V}_i, \mathbf{Y}_i\} = -\frac{1}{2\sigma_z^2}(\mathbf{y}_i - \mathbf{B}_i(\boldsymbol{\beta}, \boldsymbol{\mu}) - \mathbf{G}_i\tilde{\mathbf{X}}_i)^{\mathrm{T}} \operatorname{diag}\left(\frac{1}{\mathbf{V}_i^Z}\right)(\mathbf{y}_i - \mathbf{B}_i(\boldsymbol{\beta}, \boldsymbol{\mu}) - \mathbf{G}_i\tilde{\mathbf{X}}_i),$$

where $\tilde{\mathbf{X}}_i = \mathbf{X}_i - \mathbf{b}_i$. Thus the gradient with respect to $(\boldsymbol{\beta}, \boldsymbol{\mu})$ equals

$$\nabla_{[\beta,\mu]} L_i(\boldsymbol{\Theta}; \mathbf{Y}_i, \mathbf{V}_i, \mathbf{X}_i) = \frac{1}{\sigma_z^2} \mathbf{B}_i^{\mathrm{T}} \operatorname{diag}\left(\frac{1}{\mathbf{V}_i^Z}\right) (\mathbf{y}_i - \mathbf{B}_i(\boldsymbol{\beta}, \boldsymbol{\mu}) - \mathbf{G}_i \tilde{\mathbf{X}}_i).$$

Using that the expected value of $\mathbf{X}_i$ given $\mathbf{V}_i$ and $\mathbf{Y}_i$ is $\tilde{\mathbf{b}}_i$ (see Appendix A.1) we obtain that

$$\nabla_{(\beta,\mu)} L_i(\boldsymbol{\Theta}; \mathbf{Y}_i, \mathbf{V}_i) = \frac{1}{\sigma_z^2} \mathbf{B}_i^{\mathrm{T}} \operatorname{diag}\left(\frac{1}{\mathbf{V}_i^Z}\right) (\mathbf{y}_i - \mathbf{B}_i(\boldsymbol{\beta}, \boldsymbol{\mu}) - \mathbf{G}_i(\tilde{\mathbf{b}}_i - \mathbf{b}_i)).$$

The gradient for noise variance σ^2, of the complete log-likelihood, equals

$$\nabla_\sigma \log\{L_i(\boldsymbol{\Theta}; \mathbf{y}_i, \mathbf{X}_i, \mathbf{V}_i)\} = -\frac{m_i}{\sigma} + \frac{1}{\sigma^3} \left(\mathbf{e}_i \frac{1}{\mathbf{V}_i^Z}\right)^{\mathrm{T}} \mathbf{e}_i,$$

where m_i is the number observations of patient i and $\mathbf{e}_i = \mathbf{y}_i - \mathbf{B}_i(\boldsymbol{\beta}, \boldsymbol{\mu}) - \mathbf{G}_i \tilde{\mathbf{X}}_i$. We could compute $\nabla_\sigma \log\{L_i(\boldsymbol{\Theta}; \mathbf{y}_i, \mathbf{V}_i)\}$ by taking the expectation with respect to $\mathbf{X}_i$, but in our implementation we simply use the values of $\mathbf{X}_i$ from the Gibbs sampler to approximate this expected value by using MC integration, the reason being that the estimation of σ is so simple compared with the other parameters that it was not worth the additional effort to implement the analytical gradient for this parameter.

To derive the gradient with respect to the covariance matrix of the random effects, we first note that

$$\begin{aligned} L_i(\boldsymbol{\Sigma}; \mathbf{Y}_i, \mathbf{X}_i, \mathbf{V}_i) &= -\frac{1}{2} \log(|\boldsymbol{\Sigma}|) - \frac{1}{2V_i^U} (\mathbf{U}_i^U + (1 - V_i^U)\boldsymbol{\mu}^U)^{\mathrm{T}} \boldsymbol{\Sigma}^{-1} (\mathbf{U}_i^U + (1 - V_i^U)\boldsymbol{\mu}^U) \\ &= \frac{1}{2V_i^U} (\tilde{\mathbf{U}}_i^U)^{\mathrm{T}} \boldsymbol{\Sigma}^{-1} (\tilde{\mathbf{U}}_i^U), \end{aligned}$$

where $\tilde{\mathbf{U}}_i^U = \mathbf{U}_i^U + (1 - V_i^U)\boldsymbol{\mu}^U$. Denoting $\mathbf{M}_i = (\tilde{\mathbf{U}}_i^U)(\tilde{\mathbf{U}}_i^U)^{\mathrm{T}}$, $\mathbf{K}_{dd}$ the communication matrix and $\mathbf{D}_d$ the duplication matrix (Magnus and Neudecker (2007), pages 389–390), the gradient for the variance matrix $\boldsymbol{\Sigma}$ is

$$\nabla_{\mathrm{vech}(\boldsymbol{\Sigma})} L_i(\boldsymbol{\Theta}; \mathbf{Y}_i, \mathbf{X}_i, \mathbf{V}_i) = \frac{1}{2} \mathbf{D}_d^{\mathrm{T}} (\boldsymbol{\Sigma}^{-1} \otimes \boldsymbol{\Sigma}^{-1}) \operatorname{vec}\left(\frac{\mathbf{M}_i}{V_i^U} - \boldsymbol{\Sigma}\right).$$

Defining $\tilde{\boldsymbol{\Sigma}} = \tilde{\mathbf{Q}}_i^{-1}$ and $\tilde{\mathbf{b}} = \tilde{\mathbf{b}}_i$, the expected value equals

$$\nabla_{\mathrm{vech}(\boldsymbol{\Sigma})} L_i(\boldsymbol{\Theta}; \mathbf{Y}_i, \mathbf{V}_i) = \frac{1}{2} \mathbf{D}_d^{\mathrm{T}} (\boldsymbol{\Sigma}^{-1} \otimes \boldsymbol{\Sigma}^{-1}) \operatorname{vec}\left(\frac{\tilde{\boldsymbol{\Sigma}}_{1:d,1:d} + \tilde{\mathbf{b}}_{1:d} \tilde{\mathbf{b}}_{1:d}^{\mathrm{T}} +}{V_i^U} - \boldsymbol{\Sigma}\right).$$

For a generic parameter θ of the differential operator that is used to define the process, we have that

$$L_i(\theta; \mathbf{Y}_i, \mathbf{X}_i, \mathbf{V}_i) = \log(|\mathbf{K}|) - \tfrac{1}{2} (\mathbf{K}\mathbf{W}_i + (\mathbf{h} - \mathbf{V}_i^W)\mu^W)^{\mathrm{T}} \operatorname{diag}(\mathbf{V}_i^W)^{-1} (\mathbf{K}\mathbf{W}_i + (\mathbf{h} - \mathbf{V}_i^W)\mu^W).$$

Thus, defining $(\mathbf{K}_\theta)_{ij} = \mathrm{d}K_{ij}/\mathrm{d}\theta$, the gradient equals

$$\nabla_\theta \log\{L_i(\boldsymbol{\Theta})\} = \operatorname{tr}(\mathbf{K}_\theta \mathbf{K}^{-1}) - \mathbf{W}_i^{\mathrm{T}} \mathbf{K}_\theta^{\mathrm{T}} \operatorname{diag}(\mathbf{V}_i^W)^{-1} (\mathbf{K}\mathbf{W}_i + (\mathbf{h} - \mathbf{V}_i^W)\mu^W).$$

What remains is to compute the gradient with respect to the variance mixing parameters. For these parameters the complete log-likelihood is entirely determined by the specified distribution of the variance mixing variables. Thus there is no generic form; instead we present the three main distributions that we have considered and their resulting gradients. The three distributions are the gamma distribution with density $f(v; p, b) = \Gamma(p)^{-1} a^p v^{p-1} \exp(-av)$, the inverse Gaussian distribution with density $f(v; a, b) = b^{1/2} (2\pi)^{-1/2} v^{-3/2} \exp\{-av/2 - b/2v + \sqrt{(ab)}\}$, and the inverse gamma distribution with density $f(v; p, a) = \Gamma(p)^{-1} a^p v^{-p-1} \exp(-b/v)$. The resulting gradients for the noise parameters are given in Table 8, the random-effect parameters in Table 9 and the processes parameters in Table 10. In Tables 8–10, ψ is the digamma function and ψ_1 is the trigamma function. Note that we use a non-standard form of the t-distribution where ν is half of the degrees of freedom and the parameterization is chosen so that a sym-

Table 8. Distribution, gradient and observed Fisher information for the mixing variable of the noise

Distribution	*Distribution of* V^Z	$\nabla L_i(\nu;\mathbf{Y}_i,\mathbf{V}_i)$	$E[\nabla^2 L_i(\nu;\mathbf{Y}_i,\mathbf{V}_i)]$
t	$\mathrm{IGam}(\nu,\nu-1)$	$m_i\left\{\log(\nu-1)+\frac{\nu}{\nu-1}-\psi(\nu)\right\}-\sum_{j=1}^{m_i}\log(V_{ij}^Z)-\frac{1}{V_{ij}^Z}$	$m_i\left\{\frac{1}{\nu-1}-\psi_1(\nu)\right\}$
NIG	$\mathrm{IG}(\nu,\nu)$	$-\frac{1}{2}\left(m_i\nu^{-1}-\sum_{j=1}^{m_i}\frac{1}{V_{ij}^Z}+V_{ij}^Z-1\right)$	$\frac{m_i}{2\nu^2}$
GAL	$\mathrm{Gam}(\lambda,\lambda)$	$m_i\log(\lambda)+m_i-m_i\psi(\lambda)+\sum_{j=1}^{m_i}\log(V_{ij}^Z)-V_{ij}^Z$	$m_i\left\{\frac{1}{\lambda}-\psi_1(\lambda)\right\}$

Table 9. Distribution, gradient and observed Fisher information for the mixing variable of the random effect

Distribution	*Distribution of* V^U	$\nabla L_i(\nu;\mathbf{Y}_i,\mathbf{V}_i)$	$E[\nabla^2 L_i(\nu;\mathbf{Y}_i,\mathbf{V}_i)]$
t	$\mathrm{IGam}(\nu,\nu-1)$	$\log(\nu-1)+\frac{\nu}{\nu-1}-\psi(\nu)-\log(V_i^U)-\frac{1}{V_i^U}$	$\frac{1}{\nu-1}-\psi_1(\nu)$
NIG	$\mathrm{IG}(\nu,\nu)$	$-\frac{1}{2}\left(\nu^{-1}-\frac{1}{V_i^U}+V_i^U-1\right)$	$\frac{1}{2\nu^2}$
GAL	$\mathrm{Gam}(\lambda,\lambda)$	$\log(\lambda)+-\psi(\lambda)+\log(V_i^U)-V_i^Z$	$\frac{1}{\lambda}-\psi_1(\lambda)$

Table 10. Distribution, gradient and observed Fisher information for the mixing variable for the processes†

Distribution	*Distribution of* V^Z	$\nabla L_i(\nu;\mathbf{Y}_i,\mathbf{V}_i)$	$E[\nabla^2 L_i(\nu;\mathbf{Y}_i,\mathbf{V}_i)]$
NIG	$\mathrm{IG}(\nu,\nu h_{ij}^2)$	$-\sum_{j=1}^{n_i}\frac{1}{2}\left(\nu^{-1}-\frac{h_{ij}^2}{V_{ij}^W}+V_{ij}^W-h_{ij}\right)$	$\frac{n_i}{2\nu^2}$
GAL	$\mathrm{Gam}(h_{ij}\lambda,\lambda)$	$\sum_{j=1}^{n_i}h_{ij}\{\log(\lambda)+1\}-\psi(h_i\lambda)+h_{ij}\log(V_{ij}^U)-V_{ij}^U$	$\sum_{j=1}^{n_i}h_{ij}\left\{\frac{1}{\lambda}-\psi_1(h_{ij}\lambda)\right\}$

†Here h_{ij} is the integral of the basis function (see Appendix B).

metric version has variance 1. For $\nu<2$ this is not possible (since the variance is unbounded) and one can then instead use the parameterization $\mathrm{IGam}(\nu/2,\nu/2+1)$ which puts the mode of the IGam density at 1.

A.2.1. Joint Fisher information for mixed effects parameters

When computing Wald-type confidence intervals based on the Fisher information matrix, one should ideally compute it from the joint Hessian for all parameters. A simpler alternative which we make is to compute the joint Fisher information matrix only for the mixed effect parameters, which means that we do not take the uncertainty of the other parameters into account. This simplifies the implementation greatly and should in most scenarios have little effect since the other parameters converge much faster than the mixed effect parameters. The reason for this is that the random effects vary between individuals, so one individual can be seen as an observation whereas the other parameters receive information also from all longitudinal observations for each patient.

Let $\mathbf{\Theta}_m=(\boldsymbol{\beta},\boldsymbol{\mu},\mathrm{vech}(\mathbf{\Sigma}),\nu)$ be the vector of all parameters for a model with NIG-distributed mixed effects and let $L_i(\mathbf{\Theta}_m)$ denote the complete likelihood $L_i(\mathbf{\Theta}_m;\mathbf{Y}_i,\mathbf{V}_i,\mathbf{X}_i)$. The negative Hessian of the likelihood for patient i (the observed Fisher information is the Hessian at the mode) for these parameters can be expressed as

$$\begin{aligned}-\mathbf{H}_i=&-E_{\mathbf{V}_i}[E_{\mathbf{X}_i}[\nabla^2_{\mathbf{\Theta}_m}L_i(\mathbf{\Theta}_m)|\mathbf{Y}_i,\mathbf{V}_i]|\mathbf{Y}_i]-E_{\mathbf{V}_i}[E_{\mathbf{X}_i}[\nabla_{\mathbf{\Theta}_m}L_i(\mathbf{\Theta}_m)\nabla_{\mathbf{\Theta}_m}L_i(\mathbf{\Theta}_m)^{\mathrm{T}}|\mathbf{Y}_i,\mathbf{V}_i]|\mathbf{Y}_i]\\&+E_{\mathbf{V}_i}[E_{\mathbf{X}_i}[\nabla_{\mathbf{\Theta}_m}L_i(\mathbf{\Theta}_m)|\mathbf{Y}_i,\mathbf{V}_i]|\mathbf{Y}_i]E_{\mathbf{V}_i}[E_{\mathbf{X}_i}[\nabla_{\mathbf{\Theta}_m}L_i(\mathbf{\Theta}_m)|\mathbf{Y}_i,\mathbf{V}_i]|\mathbf{Y}_i]^{\mathrm{T}}.\end{aligned}$$

We shall now derive the inner expectations with respect to $\mathbf{X}$ (the outer are computed through MCMC sampling). We shall utilize the distribution derived for the Gibbs sampling in Appendix A.1, but for simplicity drop the index of the mean and covariance: $\tilde{\mathbf{X}} \sim N(\tilde{\mathbf{b}}+\mathbf{b}, \tilde{\mathbf{Q}}^{-1}) = N(\tilde{b}^{*}, \tilde{\boldsymbol{\Sigma}})$; going further we shall always work with the ith patient and therefore drop the index in the notation.

For the derivations, we shall need the following lemma.

Lemma 1. Let

$$\mathbf{X} = \begin{pmatrix} \mathbf{X}_A \\ \mathbf{X}_B \end{pmatrix} \sim N\left\{ \boldsymbol{\mu} = \begin{pmatrix} \boldsymbol{\mu}_A \\ \boldsymbol{\mu}_B \end{pmatrix}, \boldsymbol{\Sigma} = \begin{pmatrix} \boldsymbol{\Sigma}_{AA} & \boldsymbol{\Sigma}_{AB} \\ \boldsymbol{\Sigma}_{BB} & \boldsymbol{\Sigma}_{BB} \end{pmatrix} \right\}$$

be a d-dimensional normal distribution where A and B are subsets of $\{1, 2, \ldots, d\}$ such that $A \cup B = \{1, 2, \ldots, d\}$. Then

$$\begin{aligned} E[\mathrm{vec}(\mathbf{X}_A \mathbf{X}_A^{\mathrm{T}})\mathbf{X}_B^{\mathrm{T}}] &= E[\mathbf{X}_A \otimes \mathbf{X}_A \otimes \mathbf{X}_B^{\mathrm{T}}] \\ &= \boldsymbol{\mu}_B^{\mathrm{T}} \otimes \boldsymbol{\mu}_A \otimes \boldsymbol{\mu}_A + \boldsymbol{\mu}_A \otimes \boldsymbol{\Sigma}_{AB} + \boldsymbol{\Sigma}_{AB} \otimes \boldsymbol{\mu}_A + \mathrm{vec}(\boldsymbol{\Sigma}_{A,A})\boldsymbol{\mu}_B^{\mathrm{T}}. \end{aligned} \tag{24}$$

Proof. From corollary 2.2.7.2 in Kollo and von Rosen (2006) it follows that

$$E[\mathbf{X} \otimes \mathbf{X} \otimes \mathbf{X}^{\mathrm{T}}] = \boldsymbol{\mu}^{\mathrm{T}} \otimes \boldsymbol{\mu} \otimes \boldsymbol{\mu} + \boldsymbol{\mu} \otimes \boldsymbol{\Sigma} + \boldsymbol{\Sigma} \otimes \boldsymbol{\mu} + \mathrm{vec}(\boldsymbol{\Sigma})\boldsymbol{\mu}^{\mathrm{T}} \tag{25}$$

To link this result with equation (24) we define the two matrices, $\mathbf{B}_A$ and $\mathbf{B}_B$, such that $\mathbf{X}_A = \mathbf{B}_A \mathbf{X}$, and $\mathbf{X}_B = \mathbf{B}_B \mathbf{X}$. Now it follows that $\mathrm{vec}(\mathbf{X}_A \mathbf{X}_A^{\mathrm{T}}) = \mathrm{vec}(\mathbf{B}_A \mathbf{X}\mathbf{X}^{\mathrm{T}} \mathbf{B}_A^{\mathrm{T}}) = \mathbf{B}_A \otimes \mathbf{B}_A \mathrm{vec}(\mathbf{X}\mathbf{X}^{\mathrm{T}})$, and the left-hand side of equation (24) can be rewritten as

$$E[\mathrm{vec}(\mathbf{X}_A \mathbf{X}_A^{\mathrm{T}})\mathbf{X}_B^{\mathrm{T}}] = \mathbf{B}_A \otimes \mathbf{B}_A E[\mathbf{X} \otimes \mathbf{X} \otimes \mathbf{X}^{\mathrm{T}}]\mathbf{B}_B^{\mathrm{T}}.$$

Joining the equation above with equation (25) gives the following three terms from which we shall extract the final result:

$$\begin{aligned} (\mathbf{B}_A \otimes \mathbf{B}_A)(\boldsymbol{\mu}^{\mathrm{T}} \otimes \boldsymbol{\mu} \otimes \boldsymbol{\mu})\mathbf{B}_B^{\mathrm{T}} &= (\mathbf{B}_B \boldsymbol{\mu})^{\mathrm{T}} \otimes \mathbf{B}_A \boldsymbol{\mu} \otimes \mathbf{B}_A \boldsymbol{\mu} = \boldsymbol{\mu}_B^{\mathrm{T}} \otimes \boldsymbol{\mu}_A \otimes \boldsymbol{\mu}_A, \\ (\mathbf{B}_A \otimes \mathbf{B}_A)(\boldsymbol{\mu} \otimes \boldsymbol{\Sigma})\mathbf{B}_B^{\mathrm{T}} &= \mathbf{B}_A \boldsymbol{\mu} \otimes \mathbf{B}_A \boldsymbol{\Sigma} \mathbf{B}_B^{\mathrm{T}} = \boldsymbol{\mu}_A \otimes \boldsymbol{\Sigma}_{AB}, \\ (\mathbf{B}_A \otimes \mathbf{B}_A)(\mathrm{vec}(\boldsymbol{\Sigma})\boldsymbol{\mu}^{\mathrm{T}})\mathbf{B}_B^{\mathrm{T}} &= \mathrm{vec}(\mathbf{B}_A \boldsymbol{\Sigma} \mathbf{B}_A^{\mathrm{T}})(\mathbf{B}_B \boldsymbol{\mu})^{\mathrm{T}} = \mathrm{vec}(\boldsymbol{\Sigma}_{A,A})\boldsymbol{\mu}_B^{\mathrm{T}}. \end{aligned} \qquad \square$$

Several of the required gradients are straightforward to derive and we therefor omit most details. For example, some simple second derivatives that are needed are

$$\begin{aligned} \nabla^2_{[\beta,\mu]} L_i(\boldsymbol{\Theta}_m) &= -\frac{1}{\sigma^2}\frac{1}{V^Z}\mathbf{B}_i^{\mathrm{T}}\mathbf{B}_i, \\ \nabla^2_{\mathrm{vech}(\boldsymbol{\Sigma})} L_i(\boldsymbol{\Theta}_m) &= -\frac{1}{2}\mathbf{D}_d^{\mathrm{T}}\mathbf{K}_{dd}\left(\boldsymbol{\Sigma}^{-1} \otimes \boldsymbol{\Sigma}^{-1}\left(\frac{\mathbf{M}_i}{V_i^U} - \boldsymbol{\Sigma}\right)\boldsymbol{\Sigma}^{-1} + \boldsymbol{\Sigma}^{-1}\left(\frac{\mathbf{M}_i}{V_i^U}\right)\boldsymbol{\Sigma}^{-1} \otimes \boldsymbol{\Sigma}^{-1}\right)\mathbf{D}_d, \\ \mathrm{E}[\nabla^2_{\mathrm{vech}(\boldsymbol{\Sigma})} L_i(\boldsymbol{\Theta}_m)] &= -\frac{1}{2}\mathbf{D}_d^{\mathrm{T}}\mathbf{K}_{dd}(\boldsymbol{\Sigma}^{-1} \otimes \boldsymbol{\Sigma}^{-1})\mathbf{D}_d. \end{aligned}$$

Likewise, for the parameter of the mixing component ν, the gradient does not depend on $\mathbf{X}|\mathbf{V}$ and its expected value is hence easily evaluated from the gradient. See Tables 8, 9 and 10.

We now present the more difficult components to compute. We start with evaluating the expected value of the outer product of $\nabla_{\mathrm{vech}(\boldsymbol{\Sigma})} L_i(\boldsymbol{\Theta}_m)$ which we split into several parts. The gradient is

$$\nabla_{\mathrm{vech}(\boldsymbol{\Sigma})} L_i(\boldsymbol{\Theta}_m) = \mathbf{H}_{\Sigma}\mathrm{vec}\left(\frac{\mathbf{M}}{V^U}\right) - \mathbf{H}_{\Sigma}\mathrm{vec}(\boldsymbol{\Sigma}),$$

and thus the outer product is

$$\nabla_{\mathrm{vech}(\boldsymbol{\Sigma})} L_i(\boldsymbol{\Theta}_m) \nabla_{\mathrm{vech}(\boldsymbol{\Sigma})} L_i(\boldsymbol{\Theta}_m)^{\mathrm{T}} = \mathbf{H}_{\Sigma}(\mathbf{K}_1 - \mathbf{K}_2 - \mathbf{K}_2^{\mathrm{T}} + \mathbf{K}_3)\mathbf{H}_{\Sigma}^{\mathrm{T}},$$

where $\mathbf{K}_1 = \mathrm{vec}(\mathbf{M}_i/V_i^U)\mathrm{vec}(\mathbf{M}/V^U)^{\mathrm{T}}$, $\mathbf{K}_2 = \mathrm{vec}(\mathbf{M}/V^U)\mathrm{vec}(\boldsymbol{\Sigma})^{\mathrm{T}}$ and $\mathbf{K}_3 = \mathrm{vec}(\boldsymbol{\Sigma})\mathrm{vec}(\boldsymbol{\Sigma})^{\mathrm{T}}$. To compute the expectation of the outer product we need the expectation of $\mathrm{vec}(\mathbf{M})$ and $\mathrm{vec}(\mathbf{M})\mathrm{vec}(\mathbf{M})^{\mathrm{T}}$. First

$$E_{\mathbf{X}}\left[\frac{1}{V^U}\mathrm{vec}(\mathbf{M})|\mathbf{Y},\mathbf{V}\right]=\frac{1}{V^U}\mathrm{vec}(E_{\mathbf{X}}[\tilde{\mathbf{X}}_{1:d}\tilde{\mathbf{X}}_{1:d}^{\mathrm{T}}])=\frac{1}{V^U}\mathrm{vec}\{\tilde{\mathbf{\Sigma}}_{1:d,1:d}+\tilde{\mathbf{b}}^{*}_{1:d}(\tilde{\mathbf{b}}^{*}_{1:d})^{\mathrm{T}}\}.$$

To derive the expectation of $\mathbf{K}_1$ we use theorem 4.3 of Magnus and Neudecker (1979):

$$\begin{aligned}E_{\mathbf{X}}\left[\frac{1}{(V^U)^2}\,\mathrm{vec}(\mathbf{M})\,\mathrm{vec}(\mathbf{M})^{\mathrm{T}}|\mathbf{Y},\mathbf{V}\right]&=\frac{1}{(V^U)^2}E_{\mathbf{X}}[\tilde{\mathbf{X}}_{1:d}\tilde{\mathbf{X}}_{1:d}^{\mathrm{T}}\otimes\tilde{\mathbf{X}}_{1:d}\tilde{\mathbf{X}}_{1:d}^{\mathrm{T}}|\mathbf{Y},\mathbf{V}]\\&=\frac{1}{(V^U)^2}(\mathbf{I}+\mathbf{K}_d)(\tilde{\mathbf{\Sigma}}_{1:d,1:d}\otimes\tilde{\mathbf{\Sigma}}_{1:d,1:d}+\tilde{\mathbf{\Sigma}}_{1:d,1:d}\otimes\tilde{\mathbf{b}}^{*}_{1:d}(\tilde{\mathbf{b}}^{*}_{1:d})^{\mathrm{T}}\\&\quad+\tilde{\mathbf{b}}^{*}_{1:d}(\tilde{\mathbf{b}}^{*}_{1:d})^{\mathrm{T}}\otimes\tilde{\mathbf{\Sigma}}_{1:d,1:d})\\&\quad+E_{\mathbf{X}}\left[\frac{1}{V^U}\mathrm{vec}(\mathbf{M})|\mathbf{Y},\mathbf{V}\right]\,E_{\mathbf{X}}\left[\frac{1}{V_i^U}\mathrm{vec}(\mathbf{M})|\mathbf{Y},\mathbf{V}\right]^{\mathrm{T}},\end{aligned}$$

where $\mathbf{K}_{dd}$ again denotes the communication matrix.

We continue with the outer product of $\nabla_{[\beta,\mu]}L_i(\mathbf{\Theta}_m)$:

$$\nabla_{[\beta,\mu]}L_i(\mathbf{\Theta}_m)\nabla_{[\beta,\mu]}L_i(\mathbf{\Theta}_m)^{\mathrm{T}}=\mathbf{a}\mathbf{a}^{\mathrm{T}}-\mathbf{a}\mathbf{A}^{\mathrm{T}}\mathbf{X}^{\mathrm{T}}-\mathbf{A}\mathbf{X}\mathbf{a}^{\mathrm{T}}+\mathbf{A}\mathbf{X}\mathbf{X}^{\mathrm{T}}\mathbf{A}^{\mathrm{T}},$$

where

$$\mathbf{a}=\frac{1}{2\sigma_z^2}\mathbf{B}^{\mathrm{T}}\,\mathrm{diag}\left(\frac{1}{\mathbf{V}^Z}\right)(\mathbf{y}-\mathbf{B}[\beta,\mu])$$

and

$$\mathbf{A}=\frac{1}{2\sigma_z^2}\mathbf{B}^{\mathrm{T}}\,\mathrm{diag}\left(\frac{1}{\mathbf{V}^Z}\right)\mathbf{G}.$$

The expectations of the terms are easily obtained since $\mathbf{X}\sim N(\tilde{\mathbf{b}},\tilde{\mathbf{\Sigma}})$. To compute the expectation we typically do not compute $\tilde{\mathbf{\Sigma}}$ but rather solve linear systems using $\tilde{\mathbf{Q}}$.

The final difficulty is to compute the expectation of the outer product:

$$\begin{aligned}\nabla_{[\beta,\mu]}L_i(\mathbf{\Theta}_m)\nabla_{\mathrm{vech}(\mathbf{\Sigma})}L_i(\mathbf{\Theta}_m)^{\mathrm{T}}&=\frac{1}{2\sigma_z^2}\mathbf{B}^{\mathrm{T}}\,\mathrm{diag}\left(\frac{1}{\mathbf{V}^Z}\right)(\mathbf{Y}-\mathbf{B}(\beta,\mu)-\mathbf{G}\tilde{\mathbf{X}}_i)\mathrm{vec}\left(\frac{\mathbf{M}}{V^U}-\mathbf{\Sigma}\right)^{\mathrm{T}}\mathbf{H}_{\Sigma}^{\mathrm{T}}\\&=\tilde{\mathbf{a}}\left(-\mathrm{vec}(\mathbf{\Sigma})^{\mathrm{T}}+\frac{1}{V^U}\mathrm{vec}(\mathbf{M}_i)^{\mathrm{T}}\right)\mathbf{H}_{\Sigma}^{\mathrm{T}}+\mathbf{A}\tilde{\mathbf{X}}\left(\mathrm{vec}(\mathbf{\Sigma})^{\mathrm{T}}-\frac{1}{V^U}\mathrm{vec}(\mathbf{M})^{\mathrm{T}}\right)\mathbf{H}_{\Sigma}^{\mathrm{T}},\end{aligned}$$

where

$$\tilde{\mathbf{a}}=\mathbf{a}+\frac{1}{2\sigma_z^2}\mathbf{B}^{\mathrm{T}}\,\mathrm{diag}\left(\frac{1}{\mathbf{V}^Z}\right)\mathbf{G}\mathbf{b}.$$

For most of the terms in this expression we have already calculated the corresponding expectation before. The only new term is $\tilde{\mathbf{X}}\mathrm{vec}(\mathbf{M})^{\mathrm{T}}$, which by lemma 1 is

$$E_{\mathbf{X}}[\tilde{\mathbf{X}}\mathrm{vec}(\mathbf{M})^{\mathrm{T}}|\mathbf{Y},\mathbf{V}]=\tilde{\mathbf{b}}^{*}\otimes(\tilde{\mathbf{b}}^{*}_{1:d})^{\mathrm{T}}\otimes(\tilde{\mathbf{b}}^{*}_{1:d})^{\mathrm{T}}+(\tilde{\mathbf{b}}^{*}_{1:d})^{\mathrm{T}}\otimes\tilde{\mathbf{\Sigma}}_{.,1:d}+\tilde{\mathbf{\Sigma}}_{.,1:d}\otimes(\tilde{\mathbf{b}}^{*}_{1:d})^{\mathrm{T}}+\tilde{\mathbf{b}}^{*}\,\mathrm{vec}(\tilde{\mathbf{\Sigma}}_{1:d,1:d})^{\mathrm{T}}.$$

A.3. Similarity between densities

Finding the parameters for the GH distribution is in general difficult, because the full log-likelihood surface is largely flat, which makes the model parameters almost non-identifiable. A further difficulty is that the boundary of the parameter space often contains, unique, distributions and hence one cannot expect that the parameter will be contained in a compact region of the parameter space. This problem is also true within the subfamilies that were discussed above. For instance, an NIG distribution converges to a Cauchy distribution as $a\to 0$, and to a Gaussian distribution if $a\to\infty$ and $b\to\infty$ at the same rate. Recognizing these limiting cases is important in practice since it can lead to situations where the parameters do not converge.

A remedy for this issue within the subfamilies that we are studying is to fix a compact parameter space and if the parameters converge to the boundary then we re-estimate the parameters in the limiting distribution. We set these boundaries by examining the total variation (TV) distance between pairs of densities. For illustration, to compare a symmetric NIG distribution with fixed a with a symmetric Cauchy distribution, we calculate

$$\mathrm{TV}_{\mathrm{NIG,CH}}(b_{\mathrm{CH}}, a, b_{\mathrm{NIG}}) = \min_{b_{\mathrm{CH}}} \int |\mathrm{CH}(x; 0, 0, b_{\mathrm{CH}}) - \mathrm{NIG}(x; 0, 0, a, b_{\mathrm{NIG}})| \mathrm{d}x.$$

To simplify the calculations that are needed to find the Cauchy distribution $\mathrm{CH}(0, 0, b_{\mathrm{CH}})$ that is closest to the $\mathrm{NIG}(0, 0, a, b_{\mathrm{NIG}})$ distribution we use the following proposition, which shows that it suffices first to find the Cauchy distribution that is closest to $\mathrm{NIG}(0, 0, a, 1)$, and then to rescale the shape parameter by b_{NIG}.

Proposition 2. Let $f_s(x)$ and $g_h(x)$ be two distributions with respect to the Lebesgue measure, with scaling parameters s and h. Then, $\mathrm{TV}(f_s, g_h) = \mathrm{TV}(f_{s/c}, g_{h/c})$ for $c > 0$.

Proof. First note that

$$\mathrm{TV}(f_{s/c}, g_{h/c}) = \frac{1}{2} \int |f_{s/c}(x) - g_{h/c}(x)| \mathrm{d}x = \frac{c}{2} \int |f_s(cx) - g_h(cx)| \mathrm{d}x.$$

Now use integration by substitution with respect to $\phi(x) = x/c$ to give

$$\frac{c}{2} \int |f_s(cx) - g_h(cx)| \mathrm{d}x = \frac{1}{2} \int |f_s(x) - g_h(x)| \mathrm{d}x = \mathrm{TV}(f_s, g_h).$$

Fig. 11 shows the TV distances between the NIG and Cauchy, and between the NIG and Gaussian distributions, as functions of a. One can now translate the difference between the densities to compare with densities that one is more familiar with. For example, for $a = 0.001$, the TV distance between the NIG and Cauchy distribution is less than that between two Bernoulli distributions whose probabilities differ by 0.002. The same applies to the TV distance between the NIG and normal distributions when $a = 250$.

In ngme we set the boundaries of the NIG parameter space to $0.001 \leqslant a < 250$, and if the parameter space is hit it gives a warning. Of course one needs to be a little cautious with using the limiting distribution,

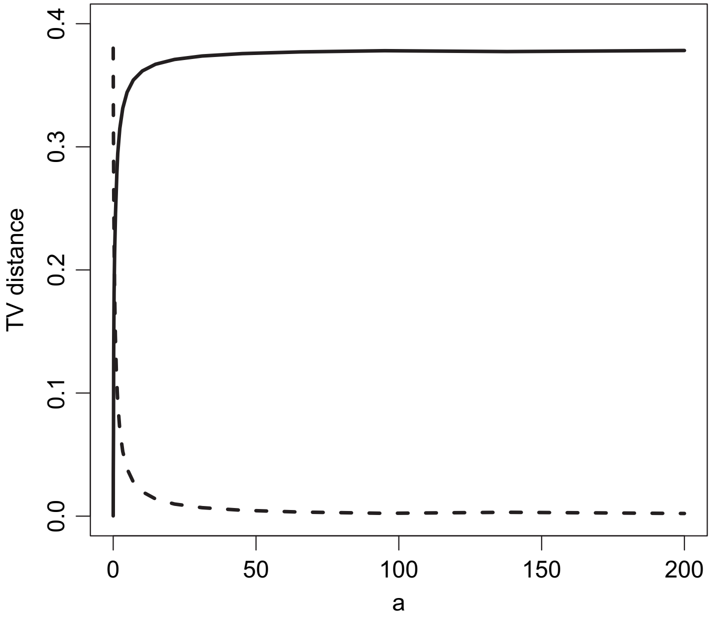

Fig. 11. TV distance between the NIG and Cauchy (– – –) and between the NIG and normal (———) distributions for varying a

since, although the TV difference decreases, the tails of the distributions remain different. For instance, the NIG distribution has exponential tails whereas the Cauchy distribution has polynomial tails.

A.4. Pseudocode for the grouped subsampler

Algorithm 1 (Table 11) contains pseudocode describing the group formation of the grouped subsampler.

Appendix B: Discretization

In this section we outline how the stochastic differential equation (13) is discretized. Let $\langle f, g\rangle = \int f(t)g(t)\mathrm{d}t$ denote the standard inner product on $\mathbb{R}$. Recall that we restrict $W(t)$ to a finite interval, $0 \leqslant t \leqslant t_{\max}$, and impose boundary conditions on the operator to obtain a well-posed problem. The so-called *weak solution* of equation (13) is a function of $W(t)$ that satisfies the equation

$$\langle \psi, \mathcal{D}W\rangle = \langle \psi, \mathrm{d}L\rangle, \tag{26}$$

for a specified set of *test functions* $\psi(t)$. Recall that we use the *low rank* approximation (14) and now want to compute the distribution of the weights in this basis expansion. When $\mathcal{D} = \kappa^2 - \partial^2/\partial t^2$, we can use a standard Galerkin finite element discretization; see also Lindgren and Rue (2008). This consists of setting all the test functions to the basis functions, i.e. $\psi_k = \phi_k$ for all k, and computing the W_k by solving the system of equations that is defined by equation (26), i.e. $\mathbf{KW} = \mathbf{L}$, where $L_k = \langle \psi_k, \mathrm{d}L\rangle$, and $\mathbf{K}$ is a discretized version of the differential operator $\mathcal{D}$ with elements

$$K_{kk'} = \langle \psi_k, \mathcal{D}\phi_{k'}\rangle = \kappa^2 \langle \psi_k, \phi_{k'}\rangle + \left\langle \frac{\partial}{\partial t}\psi_k, \frac{\partial}{\partial t}\phi_{k'} \right\rangle - \langle \psi_k, \partial_n \phi_{k'}\rangle_{\partial T}. \tag{27}$$

Table 11. Algorithm 1: group formation for the grouped subsampler

```
*procedure* Group-formation ($\mathbf{x}_1, \ldots, \mathbf{x}_m$)
    $\mathcal{I} \leftarrow \{1, \ldots, m\}$                                    $m$ is the total number of subjects to group
    $k \leftarrow 1$
    $\mathcal{G}_0 \leftarrow \emptyset$
    *while* $|\mathcal{I}| > 0$ *do*
        $\tilde{\mathcal{G}} \leftarrow$ Create-group($\mathcal{I}, \mathbf{x}_1, \ldots, \mathbf{x}_m$)
        *if* rank($\Sigma_{i\in\mathcal{G}_k} \mathbf{x}_i \mathbf{x}_i^{\mathrm{T}}$) = columns($\mathbf{x}_1$) *then*      columns($\mathbf{x}_1$) is the number of covariates
            $\mathcal{G}_k \leftarrow \tilde{\mathcal{G}}$
            $\mathcal{I} \leftarrow \mathcal{I} \setminus \mathcal{G}_k$
            $k \leftarrow k + 1$
        *else*
            $\mathcal{G}_0 \leftarrow \mathcal{I}$
            $\mathcal{I} \leftarrow \emptyset$
        *end if*
    *end while*
    *return* $\mathcal{G}_0, \ldots, \mathcal{G}_k$
*end procedure*
*procedure* Create-group($\mathcal{I}, \mathbf{x}_1, \ldots, \mathbf{x}_m$)
    $\mathcal{G} \leftarrow \mathcal{I}_1$
    $\mathcal{I} \leftarrow \mathcal{I} \setminus \mathcal{I}_1$
    *while* rank($\Sigma_{i\in\mathcal{G}} \mathbf{x}_i \mathbf{x}_i^{\mathrm{T}}$) < columns($\mathbf{x}_1$) and $|\mathcal{I}| > 0$ *do*
        *if* rank($\mathbf{x}_{\mathcal{I}_1} \mathbf{x}_{\mathcal{I}_1}^{\mathrm{T}} + \Sigma_{i\in\mathcal{G}} \mathbf{x}_i \mathbf{x}_i^{\mathrm{T}}$) > rank($\Sigma_{i\in\mathcal{G}} \mathbf{x}_i \mathbf{x}_i^{\mathrm{T}}$) *then*
            $\mathcal{G} \leftarrow \mathcal{G} \cup \mathcal{I}_1$
        *end if*
        $\mathcal{I} \leftarrow \mathcal{I} \setminus \mathcal{I}_1$
    *end while*
    *return* $\mathcal{G}$
*end procedure*
```

Here the final term vanishes if Dirichlet or Neumann boundary conditions are used.

For the NIG version of the model, we approximate the distribution of L_k by

$$L_k = h_k \delta^W + \mu^W V_k^W + \sqrt{V_k^W} Z_k,$$

where $Z_k \sim N(0, 1)$, $h_k = \langle \psi_k, 1 \rangle$ and $V_k \sim \mathrm{IG}(\nu, {h_k}^2\nu)$ (Bolin, 2014). It follows that the distribution for the stochastic weight vector $\mathbf{W}$ conditional on V can be written as equation (15).

When $\mathcal{D} = \kappa + \partial/\partial t$ is a first-order operator, we cannot use the Galerkin method. We then instead use a Petrov–Galerkin method, where the test functions above are replaced by piecewise constant functions:

$$\psi_i(t) = \begin{cases} 1, & s_i < t < s_{i+1}, \\ 0, & \text{otherwise.} \end{cases}$$

With this change, the distribution of $\mathbf{L}$ is the same as above (which is not an approximation in this case), but the elements of $\mathbf{K}$ are

$$K_{kk'} = \langle \psi_k, \mathcal{D}\phi_{k'} \rangle = \kappa \langle \psi_k, \phi_{k'} \rangle + \left\langle \psi_k, \frac{\partial}{\partial t}\phi_{k'} \right\rangle. \tag{28}$$

If the operator is an integer power of a first- or second-order operator, the model can be rewritten as a system of equations. For example $\mathcal{D}^2 W(t) = \mathrm{d}L(t)$ can be formulated as the system

$$\begin{aligned} \mathcal{D}W(t) &= u(t), \\ \mathcal{D}u(t) &= \mathrm{d}L(t). \end{aligned}$$

Both of these equations can then be discretized by using the method above. Combining the two discretizations yields the following equation for the coefficients, $\mathbf{KCKW} = \mathbf{L}$, where $\mathbf{C}$ is the mass matrix with elements $C_{kk'} = \langle \psi_k, \phi_{k'} \rangle$. If the operator is a fractional power of a first- or second-order operator, the iterative formulation cannot be used. However, the fractional power could probably still be handled by using the methods in Bolin *et al.* (2018) and Bolin and Kirchner (2019).

References

Andrieu, C., Moulines, É. and Priouret, P. (2007) Stability of stochastic approximation under verifiable conditions. *SIAM J. Control Optimizn*, **44**, 283–312.

Aralleno-Valle, R. B., Bolfarine, H. and Lachos, V. H. (2007) Bayesian inference for skew-Normal linear mixed models. *J. Appl. Statist.*, **34**, 663–682.

Asar, Ö., Ritchie, J. P., Kalra, P. A. and Diggle, P. J. (2016) Short-term and long-term effects of acute kidney injury in chronic kidney disease patients: a longitudinal analysis. *Biometr. J.*, **58**, 1552–1566.

Bai, X., Chen, K. and Yao, W. (2016) Mixture of linear mixed models using multivariate *t* distribution. *J. Statist. Computn Simuln*, **86**, 771–787.

Barndorff-Nielsen, O. E. (1977) Exponentially decreasing distributions for the logarithm of the particle size. *Proc. R. Soc.* A, **353**, 401–419.

Barndorff-Nielsen, O. (1997a) Processes of normal inverse Gaussian type. *Finan. Stochast.*, **2**, 41–68.

Barndorff-Nielsen, O. (1997b) Normal inverse Gaussian distributions and stochastic volatility modelling. *Scand. J. Statist.*, **24**, 1–13.

Bibby, B. and Sørensen, M. (2003) Hyperbolic processes in finance. In *Handbook of Heavy Tailed Distributions in Finance*, pp. 319–337. Berlin: Springer.

Bolin, D. (2014) Spatial Matérn fields driven by non-Gaussian noise. *Scand. J. Statist.*, **41**, 557–579.

Bolin, D. and Kirchner, K. (2019) The rational SPDE approach for Gaussian random fields with general smoothness. *J. Computnl Graph. Statist.*, to be published.

Bolin, D., Kirchner, K. and Kovacs, M. (2018) Numerical solution of fractional elliptic stochastic PDEs with spatial white noise. *IMA J. Numer. Anal.*

Bolin, D. and Wallin, J. (2020) Multivariate type G Matérn stochastic partial differential equation random fields. *J. R. Statist. Soc.* B, **82**, 215–239.

Cabral, C. R., Lachos, V. H. and Madruga, M. R. (2012) Bayesian analysis of skew-Normal independent linear mixed models with heterogeneity in the random-effects population. *J. Statist. Planng Inf.*, **142**, 181–200.

Chang, S.-C. and Zimmerman, D. L. (2016) Skew-Normal antedependence models for skew longitudinal data. *Biometrika*, doi 10.1093/biomet/asw006.

Choudhary, P. K., Sengupta, D. and Cassey, P. (2014) A general skew-*t* mixed model that allows different degrees of freedom for random effects and error distribution. *J. Statist. Planng Inf.*, **147**, 235–247.

Davies, J. C. and Alton, E. W. (2009) Monitoring respiratory disease severity in cystic fibrosis. *Resp. Med.*, **54**, 606–617.

Davidian, M. and Gallant, A. R. (1993) The nonlinear mixed effects models with a smooth random effects density. *Biometrika*, **80**, 475–488.

De la Cruz, R. (2014) Bayesian analysis for nonlinear mixed-effects models under heavy-tailed distributions. *Pharmceut. Statist.*, **13**, 81–93.

Dempster, A. P., Laird, N. M. and Rubin, D. B. (1977) Maximum likelihood from incomplete data via the EM algorithm (with discussion). *J. R. Statist. Soc.* B, **39**, 1–38.

Diggle, P. J. (1988) An approach to the analysis of repeated measurements. *Biometrics*, **44**, 959–971.

Diggle, P. J., Heagerty, P. J., Liang, K.-Y. and Zeger, S. L. (1994) *Analysis of Longitudinal Data*. Oxford: Oxford University Press.

Diggle, P. J., Heagerty, P. J., Liang, K.-Y. and Zeger, S. L. (2002) *Analysis of Longitudinal Data*, 2nd edn. Oxford: Oxford University Press.

Diggle, P. J., Sousa, I., and Asar, Ö. (2015) Real-time monitoring of progression towards renal failure in primary care patients. *Biostatistics*, **16**, 522–536.

Eberlein, E. (2001) Application of generalized hyperbolic Lévy motions to finance. In *Lévy Processes: Theory and Applications*, pp. 319–337.

Fitzmaurice, G. M., Laird, N. M., and Ware, J. H. (2011) *Applied Longitudinal Analysis*, 2nd edn. Hoboken: Wiley.

Ghidey, W., Lesaffre, E. and Eilers, P. (2004) Smooth random effects distribution in a linear mixed model. *Biometrics*, **60**, 945–953.

Henderson, R., Diggle, P. and Dobson, A. (2000) Joint modelling of longitudinal measurements and event time data. *Biostatistics*, **1**, 465–480.

Ho, H. L. and Lin, T.-I. (2010) Robust linear mixed models using the skew *t* distribution with application to schizophrenia data. *Statist. Med.*, **52**, 449–469.

Jara, A., Quintana, F. and Martín, E. S. (2008) Linear mixed models with skew-elliptical distributions: a Bayesian approach. *Computnl Statist. Data Anal.*, **52**, 5033–5045.

Jennrich, R. I. and Schluchter, M. D. (1986) Unbalanced repeated-measures models with structured covariance matrices. *Biometrics*, **42**, 805–820.

Jørgensen, B. (1982) *Statistical Properties of the Generalized Inverse Gaussian Distribution*, pp. 401–419. Berlin: Springer.

Kay, S. R., Fiszbein, A. and Opler, L. A. (1987) The Positive and Negative Syndrome Scale (PANSS) for schizophrenia. *Schiz. Bull.*, **13**, 261–276.

Kazemi, I., Mahdiyeh, Z., Mansourian, M. and Park, J. J. (2013) Bayesian analysis of multivariate mixed models for a prospective cohort study using skew-elliptical distributions. *Biometr. J.*, **55**, 495–508.

Kleinman, K. P. and Ibrahim, J. G. (1998) A semiparametric Bayesian approach to the random effects model. *Biometrics*, **54**, 921–938.

Koller, M. (2016) robustlmm: an R package for robust estimation of linear mixed-effects models. *J. Statist. Softwr.*, 1–24.

Koller, M. and Stahel, W. A. (2016) Nonsingular subsampling for regression S estimators with categorical predictors. *Computnl Statist.*, 1–16.

Kollo, T. and von Rosen, D. (2006) Advanced multivariate statistics with matrices. In *Mathematics and Its Applications*. Springer.

Kushner, H. and Yin, G. (2003) *Stochastic Approximation and Recursive Algorithms and Applications*. Berlin: Springer.

Lachos, V. H., Castro, L. M. and Dey, D. K. (2013) Bayesian inference in nonlinear mixed-effects models using Normal independent distributions. *Computnl Statist. Data Anal.*, **64**, 237–252.

Lachos, V. H., Bandyopadhyay, D. and Dey, D. K. (2011) Linear and nonlinear mixed-effects models for censored HIV viral loads using Normal/independent distributions. *Biometrics*, **67**, 1594–1604.

Lachos, V. H., Cabral, C. R. B. and Abanto-Valle, C. A. (2012) A non-iterative sampling Bayesian method for linear mixed models with Normal independent distributions. *J. Appl. Statist.*, **39**, 531–549.

Lachos, V. H., Dey, D. K. and Cancho, V. G. (2009) Robust linear mixed models with skew-Normal independent distributions from a Bayesian perspective. *J. Statist. Planng Inf.*, **139**, 4098–4110.

Lachos, V. H., Ghosh, P. and Arellano-Valle, R. B. (2010) Likelihood based inference for skew-Normal independent linear mixed models. *Statist. Sin.*, **20**, 302–322.

Laird, N. M. and Ware, J. H. (1982) Random-effects models for longitudinal data. *Biometrics*, **38**, 963–974.

Lange, K. (1995) A gradient algorithm locally equivalent to the EM algorithm. *J. R. Statist. Soc.* B, **57**, 425–437.

Lange, K. L., Little, R. J. A. and Taylor, J. M. G. (1989) Robust statistical modeling using the *t* distribution. *J. Am. Statist. Ass.*, **84**, 881–896.

Lange, K. and Sinsheimer, J. S. (1993) Normal/independent distributions and their applications in robust regression. *J. Computnl Graph. Statist.*, **2**, 175–198.

Levey, A. S., Bosch, J. P., Lewis, J. B., Greene, T., Rogers, N. and Roth, D. (1999) A more accurate method to estimate glomerular filtration rate from serum creatinine: a new prediction equation. *Ann. Intern. Med.*, **130**, 461–470.

Liang, K.-Y. and Zeger, S. L. (1986) Longitudinal data analysis using generalized linear models. *Biometrika*, **73**, 13–22.

Lin, T. I. and Lee, J. C. (2007) Bayesian analysis of hierarchical linear mixed modeling using the multivariate t distribution. *J. Statist. Planng Inf.*, **137**, 484–495.

Lin, T. I. and Lee, J. C. (2008) Estimation and prediction in linear mixed models with skew-Normal random effects for longitudinal data. *Statist. Med.*, **27**, 1490–1507.

Lin, T.-I. and Wang, W. L. (2011) Bayesian inference in joint modelling of location and scale parameters of the *t* distribution for longitudinal data. *J. Statist. Planng Inf.*, **141**, 1543–1553.

Lin, T.-I. and Wang, W. L. (2013) Multivariate skew-Normal linear mixed models for multi-outcome longitudinal data. *Statist. Modllng*, **13**, 199–221.

Lindgren, F. and Rue, H. (2008) On the second-order random walk model for irregular locations. *Scand. J. Statist.*, **35**, 691–700.

Lindgren, F., Rue, H. and Lindström, J. (2011) An explicit link between Gaussian fields and Gaussian Markov random fields: the stochastic partial differential equation approach (with discussion). *J. R. Statist. Soc.* B, **73**, 423–498.

Liu, C. and Rubin, D. B. (1995) ML estimation of the *t* distribution using EM and its extensions, ECM and ECME. *Statist. Sin.*, **5**, 19–39.

Louis, T. A. (1982) Finding the observed information matrix when using the EM algorithm. *J. R. Statist. Soc.* B, **44**, 226–233.

Lu, Z. and Zhang, Z. (2014) Robust growth mixture models with non-ignorable missingness: models, estimation, selection, and application. *Computnl Statist. Data Anal.*, **71**, 220–240.

Magnus, J. R. and Neudecker, H. (1979) The commutation matrix: some properties and applications. *Ann. Statist.*, **7**, 381–394.

Magnus, J. R. and Neudecker, H. (2007) *Matrix Differential Calculus with Applications in Statistics and Econometrics*, 3rd edn. Chichester: Wiley.

Matérn, B. (1960) *Spatial Variation*. Stockholm: Statens Skogsforsningsinstitut.

Matheson, J. and Winkler, R. (1976) Scoring rules for continuous probability distributions. *Mangmnt Sci.*, **22**, 1087–1096.

Matos, L. A., Prates, M. O., Chen, M.-H. and Lachos, V. H. (2013) Likelihood-based inference for mixed-effects models with censored response using the multivariate-t distribution. *J. Computnl Graph. Statist.*, **10**, 249–276.

Meza, C., Osorio, F. and De la Cruz, R. (2012) Estimation in nonlinear mixed-effects models using heavy-tailed distributions. *Statist. Comput.*, **22**, 121–139.

Molenberghs, G. and Verbeke, G. (2005) *Models for Discrete Longitudinal Data*. New York: Springer.

Osorio, F. (2016) heavy: robust estimation using heavy-tailed distributions. *R Package Version 0.3*. (Available from `http://cran.r-project.org/package=heavy`.)

Papaspiliopoulos, O., Roberts, G., and Sköld, M. (2007) A general framework for the parametrization of hierarchical models. *Statist. Sci.*, **1**, 59–73.

Pinheiro, J. C., Liu, C. and Wu, Y. N. (2001) Efficient algorithms for robust estimation in linear mixed-effects models using the multivariate t distribution. *J. Computnl Graph. Statist.*, **10**, 249–276.

Podgórski, K. and Wallin, J. (2016) Convolution-invariant subclasses of generalized hyperbolic distributions. *Communs Statist. Theory Meth.*, **45**, 98–103.

Riquelme, M., Bolfarine, H. and Galea, M. (2015) Robust linear functional model. *J. Multiv. Anal.*, **134**, 82–98.

Rizopoulos, D. (2012) *Joint Models for Longitudinal and Time-to-event Data: with Applications in R*. Boca Raton: Chapman and Hall–CRC.

Rosa, G. J. M., Gianola, D. and Padovani, C. R. (2004) Bayesian longitudinal data analysis with mixed models and thick-tailed distributions using MCMC. *J. Appl. Statist.*, **31**, 855–873.

Rosa, G. J. M., Padovani, C. R. and Gianola, D. (2003) Robust linear mixed models with Normal/independent distributions and Bayesian MCMC implementation. *Biometr. J.*, **45**, 573–590.

Smith, D. M. and Diggle, P. J. (1998) Compliance in an anti-hypertension trial: a latent process model for binary longitudinal data. *Statist. Med.*, **17**, 357–370.

Song, P. X.-K., Zhang, P. and Qu, A. (2007) Maximum likelihood inference in robust linear mixed-effects linear mixed effects models using multivariate t distributions. *Statist. Sin.*, **17**, 929–943.

Stirrup, O. T., Babiker, A. G., Carpenter, J. R. and Copas, A. J. (2015) Fractional Brownian motion and multivariate-t models for longitudinal biomedical data, with application to CD4 counts in HIV-patients. *Statist. Med.*, doi: 10.1002/sim.6788.

Subtil, F. and Rabilloud, M. (2010) Robust non-linear mixed modelling of longitudinal PSA levels after prostate cancer treatment. *Statist. Med.*, **29**, 573–587.

Sun, J., Frees, E. W. and Rosenberg, M. A. (2008) Heavy-tailed longitudinal modeling using copulas. *Insur. Math. Econ.*, **42**, 817–830.

Tankov, P. (2003) *Financial Modelling with Jump Processes*. Boca Raton: Chapman and Hall–CRC.

Tao, H., Palta, M., Yandell, B. S. and Newton, M. A. (2004) An estimation method for the semiparametric mixed effects model. *Biometrics*, **55**, 102–110.

Taylor, J. M. G., Cumberland, W. G. and Sy, J. P. (1994) A stochastic process model for analysis of longitudinal AIDS data. *J. Am. Statist. Ass.*, **89**, 727–736.

Taylor-Robinson, D., Whitehead, M., Diderichsen, F., Olesen, H. V., Pressler, T., Smyth, R. L. and Diggle, P. J. (2012) Understanding the natural progression in %FEV decline in patients with cystic fibrosis: a longitudinal study. *Thorax*, **67**, 860–866.

Tian, G.-L., Ng, K. W. and Tan, M. (2008) EM-type algorithms for computing restricted MLEs in multivariate Normal distributions and multivariate *t*-distributions. *Computnl Statist. Data Anal.*, **52**, 4768–4778.

Verbeke, G. and Lesaffre, E. (1996) A linear mixed-effects model with heterogeneity in the random-effects population. *J. Am. Statist. Ass.*, **91**, 217–221.

Verbeke, G. and Molenberghs, G. (2001) *Linear Mixed Models for Longitudinal Data*. New York: Springer.

Vilca, F., Balakrishnan, N. and Zeller, C. B. (2014) Multivariate skew-Normal generalized hyperbolic distribution and its properties. *J. Multiv. Anal.*, **128**, 74–85.

Vock, D. M., Davidian, M. and Tsiatis, A. A. (2012) Mixed model analysis of censored longitudinal data with flexible random-effects density. *Biostatistics*, **13**, 61–73.

Wahba, G. (1990) *Spline Models for Observational Data*. Philadelphia: Society for Industrial Mathematics.

Wallin, J. and Bolin, D. (2015) Geostatistical modelling using non-Gaussian Matérn fields. *Scand. J. Statist.*, **42**, 872–890.

Wang, W.-L. and Fan, T.-H. (2011) Estimation in multivariate *t* linear mixed models for multiple longitudinal data. *Statist. Sin.*, **21**, 1857–1880.

Wang, W.-L. and Fan, T.-H. (2012) Bayesian analysis of multivariate *t* linear mixed models using a combination of IBF and Gibbs sampler. *J. Multiv. Anal.*, **105**, 300–310.

Wang, W.-L., Lin, T.-I. and Lachos, V. H. (2015) Extending multivariate-t linear mixed models for multiple longitudinal data with censored responses and heavy tails. *Statist. Meth. Med. Res.*, doi, 10.1177/0962280215620229.

Yavuz, F. G. and Arslan, O. (2016) Linear mixed model with Laplace distribution (LLMM). *Statist. Pap.*, doi 10.1007/s00362-016-0763-x.

Zeller, C. B., Labra, F. V., Lachos, V. H. and Balakrishnan, N. (2010) Influence analyses of skew-Normal/independent linear mixed models. *Computnl Statist. Data Anal.*, **54**, 1266–1280.

Zhang, D. and Davidian, M. (2001) Linear mixed models with flexible distributions of random effects for longitudinal data. *Biometrics*, **57**, 795–802.

Zhang, Z., Lai, K., Lu, Z. and Tong, X. (2003) Bayesian inference and application of robust growth curve models using Student's t distribution. *Struct. Equn Modlng*, **20**, 47–78.

Zhang, P., Qui, Z., Fu, Y. and Song, P. X.-K. (2009) Robust transformation mixed-effects models for longitudinal continuous proportional data. *Can. J. Statist.*, **37**, 266–281.

Zhang, J., Yu, B., Zhang, L., Roskos, L., Richman, L. and Yang, H. (2015) Non-Normal random effects models for immunogenicity assay cut point determination. *J. Biopharm. Statist.*, **25**, 295–306.

Zhu, B. and Dunson, D. B. (2017) Bayesian functional data modeling for heterogeneous volatility. *Baysn Anal.*, **12**, 335–350.

Zhu, B., Song, P. X.-K. and Taylor, J. M. G. (2011a) Stochastic functional data analysis: a diffusion model-based approach. *Biometrics*, **67**, 1295–1304.

Zhu, B., Taylor, J. M. G. and Song, P. X.-K. (2011b) Semiparametric stochastic modeling of the rate function in longitudinal studies. *J. Am. Statist. Ass.*, **106**, 1485–1495.